### Title

Catalytic Cycle of Neisseria meningitidis CMP-Sialic Acid Synthetase Illustrated by High-Resolution Protein Crystallography




### Journal

Biochemistry, 59(34)

### ISSN

0006-2960



### Authors

Matthews, Melissa M
McArthur, John B
Li, Yanhong
et al.



### Publication Date

2020-09-01

### DOI

10.1021/acs.biochem.9b00517

Peer reviewed

# Catalytic cycle of *Neisseria meningitidis* CMP-sialic acid synthetase illustrated by high-resolution protein crystallography

| | |
|---|---|
| Journal: | *Biochemistry* |
| Manuscript ID | bi-2019-005179.R1 |
| Manuscript Type: | Article |
| Date Submitted by the Author: | n/a |
| Complete List of Authors: | Matthews, Melissa; University of California, Davis, Chemistry<br>McArthur, John; University of California Davis<br>Li, Yanhong; University of California Davis, Chemistry<br>Yu, Hai; University of California Davis, Chemistry<br>Chen, Xi; University of California Davis, Chemistry<br>Fisher, Andrew; University of California Davis, Chemistry |
| | |

# Catalytic cycle of *Neisseria meningitidis* CMP-sialic acid synthetase illustrated by high-resolution protein crystallography

**Melissa M. Matthews[1#], John B. McArthur[1], Yanhong Li[1], ~~John B. McArthur[1],~~ Hai Yu[1], Xi Chen[1,*], Andrew J. Fisher[1,2,*]**

[1]Department of Chemistry, University of California, Davis, CA 95616; [2]Department of Molecular and Cellular Biology, University of California, Davis, CA 95616

Running title: *Catalytic cycle of NmCSS illustrated by structures*

[#]Present address: Molecular Cryo-Electron Microscopy Unit, Okinawa Institute of Science and Technology, Onna-son, Okinawa, Japan 904-0495

*Corresponding Authors Andrew J. Fisher: ajfisher@ucdavis.edu; and Xi Chen: xiichen@ucdavis.edu

**Keywords:** carbohydrate, chemoenzymatic synthesis, crystal structure, CMP-sialic acid, CMP-sialic acid synthetase, sialic acid

## ABSTRACT

Cytidine 5'-monophosphate (CMP)-sialic acid synthetase (CSS) is an essential enzyme involved in the biosynthesis of carbohydrates and glycoconjugates containing sialic acids, a class of α-keto acids that are ~~commonly~~ generally terminal key recognition residues by many proteins that play important biological and pathological roles. The CSS from *Neisseria meningitidis* (NmCSS) has been commonly used with other enzymes such as sialic acid aldolase and/or sialyltransferase in synthesizing a diverse array of compounds containing sialic acid or its naturally occurring and non-natural derivatives. To better understand its catalytic mechanism and substrate promiscuity, four NmCSS crystal structures trapped at various stages of the catalytic cycle with bound substrates, substrate analogs, and products have been obtained and are presented here. These structures suggest a mechanism for an "open" and "closed" conformational transition that occurs as sialic acid binds to the NmCSS:CTP complex. The closed conformation positions critical residues to help facilitate the nucleophilic attack of sialic acid C2-OH to the α-phosphate of CTP, which is also aided by two observed divalent cations. Product formation drives the active site opening, promoting release of products.

## INTRODUCTION

Sialic acid-containing glycoconjugates and oligosaccharides play important roles in human biology and pathology.[1] The key enzymes for the synthesis of these structures are sialyltransferases, which use cytidine-5'-monophosphate-*N*-acetylneuraminic acid (CMP-Neu5Ac), the activated sugar nucleotide, as a donor substrate.[2] CMP-sialic acid synthetases (CSSs)[3, 4] catalyze the activation of the beta anomer of the free *N*-acetylneuraminic acid (Neu5Ac) to form a beta-linked sialyl monophosphate diester bond between the C-2 of the Neu5Ac and the alpha-phosphate of the cytidine-5'-triphosphate (CTP) and cleave off pyrophosphate (Scheme 1).

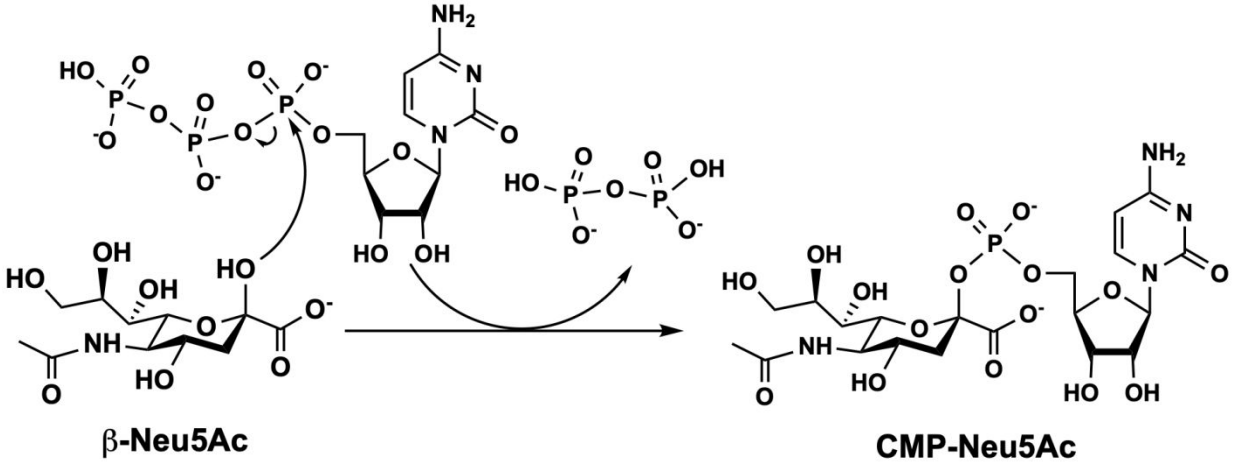


Scheme 1. Reaction catalyzed by CMP-sialic acid synthetases (CSSs).

Chemoenzymatic synthetic strategies, which combine chemical synthesis of modified monosaccharides and enzyme-catalyzed activation and transfer of sialic acid and derivatives with or without a sialic acid aldolase-catalyzed reaction, have been proven to be effective strategies for synthesizing sialosides containing natural and non-natural occurring modifications.[5, 6] CSSs from different sources have been used together with sialic acid aldolases and/or sialyltransferases for the synthesis of CMP-sialic acids, sialic acid-containing molecules, and their derivatives.[7-12] Comparing to several recombinant bacterial CSSs such as those from *Escherichia coli* K1

(EcCSS),[7, 13] *Streptococcus agalactiae* serotype V (SaVCSS),[7, 14] *Pasteurella multocida* strain P-1059 (PmCSS), *Haemophillus ducreyi* (HdCSS),[12] and *Clostridium thermocellum* (CtCSS),[15] *Neisseria meningitidis* serogroup B CSS (NmCSS)[7, 12] has been proven to be an excellent choice for synthetic applications due to its high expression level (100 mg/L culture), high activity ($k_{cat}/K_m$ = 86 $s^{-1}$ $mM^{-1}$), and promiscuous substrate specificity. It is also active in a broad pH range (7.0–10.0).[7, 12] It has been used in gram-scale synthesis of sialosides,[16, 17] and has a great potential for industrial scale synthesis. In addition to its native substrate Neu5Ac, NmCSS has been shown to tolerate substrate substitutions at the *N*-acetyl group, C-5, C-7, and C-9.[7, 12, 18, 19] Its toleration toward modifications at C-8,[12, 19, 20] however, is limited.

Previous structures of NmCSS with and without ~~the~~ a ~~inhibitor~~ cytidine-5'-diphosphate (CDP)~~,~~ inhibitor,[21] mouse CSS catalytic domain,[22] and the homologous *E. coli* cytidine-5'-diphosphate 2-keto-3-deoxy-D-manno-octulosonic acid (CMP-Kdo) synthetase,[23, 24] suggest that the enzyme, which exists as a homodimer, rotates about a central dimerization interface upon binding of sialic acid, forming an activated, "closed" state. However, ~~until now,~~ there has been no conclusive evidence for or structures illustrating the proposed closed state. All interactions between sialic acid and the homodimer have only been inferred through mutagenesis-coupled kinetics experiments,[25] or estimated through docking and modeling software.[21, 25, 26] Mechanistically, the presence of a conserved DXD motif suggests a role for divalent cations in substrate binding and mechanism. One or two cations have been observed in other CMP-transferases,[23, 27] and studies have suggested experimentally that $Mg^{2+}$ is essential for catalysis;[28] however, the precise role and location of $Mg^{2+}$ is unknown. Here four crystal structures of NmCSS are presented including one in the absence of substrate, one with CTP and two calcium ions bound, one with product CMP-Neu5Ac bound, and one with CMP plus a Neu5Ac analog, 2-deoxy-2,3-~~di~~dehydro-*N*-acetylneuraminic acid

(Neu5Ac2en). These structures provide the molecular framework of NmCSS conformational changes that occur through the catalytic cycle. The discovery of Neu5Ac2en as an NmCSS inhibitor may lead to the development of improved and selective inhibitors against bacterial CSSs as important chemical biological probes and potential therapeutics.

## MATERIALS AND METHODS

### *Expression and purification of $His_6$-tagged NmCSS*

*Neisseria meningitidis* CMP-sialic acid synthetase (NmCSS) (UniProt Accession ID: P0A0Z8) was expressed and purified as described previously,[7] with the following exceptions: cells were lysed using a microfluidizer instead of lysozyme and DNaseI, and lysate was clarified in a Beckman Avanti J-20 centrifuge using the J-20 rotor at 14,000rpm for 40 minutes before loading on the Ni-NTA column. NmCSS can routinely be purified to >95% purity at yields of up to 175mg/L of cell culture.

### *Crystallization of CSS complexes*

Crystals of CSS:CMP-sialic acid complex and substrate-free CSS were grown at room temperature by sitting-drop vapor-diffusion. A volume of 1µL protein solution containing 10mg/mL of CSS, 8mM CTP, and 8mM Neu5Ac was mixed with 1µL of reservoir (0.16M calcium acetate, 0.08M sodium cacodylate pH 6.5, 14.4% PEG 8000, and 20% glycerol). After a month of crystal growth, a single crystal was flash-cooled in liquid nitrogen. The resultant structure revealed that the product, CMP-Neu5Ac, occupied the active site along with a calcium ion in an octahedral coordination geometry. The presence of the product was surprising since it was previously thought that CSS could only use $Mg^{2+}$ to catalyze the formation of a product.[28] Although it is possible that trace $Mg^{2+}$ could have been present in the crystallization buffer, the ~~octahedral coordination geometry and~~ longer ligand distances between 2.3–2.6 Å of the metal ion suggest that it was

calcium instead of magnesium, which has typical ligand distances of ~2.2 Å.[29, 30] Presumably when given a month to react during crystal growth, CSS catalyzed the reaction with the non-preferred cation, $Ca^{2+}$. Eight-month-old crystals from this same drop were soaked in $MgCl_2$ (250 mM) for thirty minutes to try to replace $Ca^{2+}$ with the preferred $Mg^{2+}$ before flash-cooling in liquid nitrogen. However, rather than yielding the desired $Mg^{2+}$:CMP-Neu5Ac structure, diffraction data showed no electron density for any ligand in the active site of these crystals. The crystal structure determined under these conditions is presented here as the ligand-free structure.

Crystals of NmCSS:CTP were grown at room temperature by sitting-drop vapor-diffusion. A volume of 1 µL of protein mixture containing NmCSS (15 mg/mL), CTP (1 mM), and Neu5Ac (1 mM) was mixed with 1 µL of reservoir (0.1 M imidazole pH 8.0, 6% PEG 8000, and 0.2 M calcium acetate) and allowed to equilibrate. Twenty-four hours later, rectangular crystals were observed. Assuming that catalysis in the presence of $Ca^{2+}$ would be significantly slower than with $Mg^{2+}$, shortly after crystals were observed, a single crystal was selected and moved into immersion oil prior to flash-cooling in liquid nitrogen. It was anticipated that crystals flash-cooled shortly after nucleation (~24 hours), ~~that~~ the presence of $Ca^{2+}$ rather than $Mg^{2+}$ might inhibit or slow the enzyme catalysis enough during crystallization to trap a CTP plus ~~sialic acid~~Neu5Ac in a "Michalis-like" complex. However, only electron density for CTP was seen in the active site.

Crystals of NmCSS:CMP:Neu5Ac2en were grown at room temperature using hanging-drop vapor-diffusion. A volume of 200 nL of a protein solution containing NmCSS (15 mg/mL), CTP (1 mM), Neu5Ac2en (10 mM), and $MgCl_2$ (100 mM) was mixed with 200 nL of reservoir (0.1 M sodium citrate/citric acid, pH 5.5, and 20% PEG 3000). After three days of equilibration, thick-needle-shaped crystals were observed. A single crystal was selected and transferred to a cryogenic solution containing 30% ethylene glycol before being flash-cooled in liquid nitrogen. This

structure resulted in electron density that clearly defines CMP and Neu5Ac2en, suggesting that the presence of $Mg^{2+}$ allowed for the hydrolysis of CTP to CMP, and ~~afterwards~~ Neu5Ac2en bound in the active site with CMP.

In an effort to obtain a true pre-catalytic structure, experiments for co-crystallizing NmCSS with the non-hydrolyzable CTP analog cytidine-5'-[(α,β)-methyleno]triphosphate (CMPCPP), Neu5Ac, and $Mg^{2+}$ were also attempted. Although crystals diffracted well, no electron density for the analog was observed in the active site.

***Data collection, processing, and structure refinement***

Data for the substrate-free crystal were collected on beamline 24-ID-C at the Advanced Photon Source (APS) at Argonne National Laboratory. Data for all protein:substrate complexes were collected on beamline 7-1 at the Stanford Synchrotron Radiation Lightsource (SSRL). All X-ray diffraction data intensities were processed with XDS.[31] Scaling for the ligand-free enzyme-only and NmCSS:CMP-sialic acid complex was done using AIMLESS (CCP4),[32] and scaling for NmCSS:CTP and NmCSS:CMP-Neu5Ac2en was done using the program XSCALE.[31] The previously published NmCSS structure[21] (PDBID: 1EYR) was used as a model for molecular replacement in CCP4 to solve the phases for all data sets. Data collection and refinement statistics are summarized in **Table 1**.

The molecular replacement solution for the NmCSS:CMP:Neu5Ac2en structure was initially difficult to interpret because of poor electron density. To resolve this issue, the NmCSS molecular replacement model monomer was broken up into two separate domains. Domain A was made up of residues 1–138 and 170–225 (nucleotide binding domain), and domain B of residues 139–169 (dimerization domain). The two subunits were used as ensembles in PHASER[33] for an initial

round of molecular replacement. The resultant molecular replacement solution had a much improved, interpretable electron density map and revealed more of the closure between the two domains. All models were refined with REFMAC5 (CCP4)[34] and PHENIX.[35]

***Citrate activation assay***

~~***Citrate Activation Assay***~~

A 20-μL reaction mixture containing NmCSS (20 ng), $MgCl_2$ (10 mM), Tris-HCl (100 mM, pH 8.5), CTP (1 mM), Neu5Ac (1 mM), and sodium citrate (0, 1, 5, 10, or 20 mM) was incubated at 37°C in duplicate for 10 minutes. The reaction was stopped with 20 μL of pre-cooled ethanol and analyzed by capillary electrophoresis according to a previously-reported protocol.[12] The experiment was repeated on a separate day and all percent conversion values were averaged for each concentration of citrate.

***NmCSS mutagenesis and activity assays***

NmCSS mutants E162A (forward primer: 5'-GCCCAGCCTCGCCAACAATTACC-3' and reverse primer: 5'-CAAATCGCTTAGATGGCGCATGGG-3'), E162Q (Forward Primer: 5'-CAGCAGCCTCGCCAACAATTACCTCAGG-3' and reverse primer was the same as that for the E162A mutant), and R165A (forward primer: 5-GCCCAACAATTACCTCAGGCATTTAGGC-3' and reverse primer: 5'AGGCTGCTCCAAATCGCTTAGATGG-3') were prepared by Q5 site-directed mutagenesis, expressed in 50 mL cultures, and purified by Ni-NTA chromatography. For assays, a 40-μL reaction mixture containing NmCSS (4 ng) or its mutant (50 ng of E162A or E162Q, or 5 μg of R165A), $MgCl_2$ (10 mM), Tris-HCl (100 mM, pH 8.5), CTP (3 mM), Neu5Ac (1 mM) was incubated at 37 °C in duplicate for 30 minutes. The reaction was stopped with 40 μL of pre-cooled methanol and quantified with an Infinity 1290-II HPLC equipped with a UV-Vis

detector (Agilent Technologies, CA) and a CarboPac PA100 anion exchange column (Dionex), using a gradient from 0% to 90% 2 M ammonium acetate, pH 6.0, over 10 minutes against water.

***Neu5Ac2en and calcium chloride inhibition assays***

For Neu5Ac2en and calcium chloride inhibition assays, reactions were carried out at 37 °C for 30 minutes in 40-μL reaction mixtures containing CTP (3 mM), Neu5Ac (2 mM), NmCSS (8 ng), $MgCl_2$ (10 mM), and Tris-HCl buffer (100 mM, pH 8.5) with or without Neu5Ac2en (0, 0.01, 0.02, 0.05, 0.1, 0.2, 0.5, 1, 2, 5, 10 mM) or $CaCl_2$ (0, 5, 10, 20, 50, or 100 mM). The reactions were quenched and analyzed similarly to that described for the mutant assays. Data were analyzed using Grafit 5.0.

## RESULTS

### *Overall structure*

The ligand-free structure crystallizes with one monomer in the asymmetric unit with the crystallographic 2-fold generating the biologically functional dimer. The ligand-free structure presented here has an improved resolution (1.75 Å) compared to the formerly published NmCSS ligand-free structure (2.00 Å) (PDBID: 1EZI).[21] The two structures superimpose with a 0.70 Å RMSD for all 216 modelled equivalent alpha-carbons. NmCSS exists as a homodimer where each monomer is composed of a globular nucleotide-binding domain and an extended dimerization domain (Figure 1A). The dimerization domain comprises a ~35 residue insert corresponding to residues 136–171 and "domain-swaps" with the dimerization domain of the crystallographic related monomer to generate a tightly entwined complex. Improved resolution and more favorable crystal contacts allowed us to resolve the structure of the loop between αD and αE (residues 71–80), which was disordered in the previously published ligand-free structure (PDBID: 1EZI).[21] The

carbon backbone of the P-loop (residues 12–22) (~~Supplemental~~ Figure S1) was visible in the electron density, but the side-chain density for Lys16 was poor and was modeled as an alanine stub. The average B-value for this region remains high at 68.7 $Å^2$, compared to an average B-value of 28.5 $Å^2$ for the entire structure.

***Structure of NmCSS Calcium-CTP complex***

The NmCSS Calcium-CTP complex crystallized with a dimer in the asymmetric unit, and the structure was determined to 1.8 Å resolution. Many residues involved in nucleotide binding were elucidated in the NmCSS:CDP structure published previously (PDBID: 1EYR).[21] However, the NmCSS:CDP structure revealed two conformations of the diphosphate moiety of CDP, resulting in ambiguity of understanding how Mg:CTP binds and the relative orientation and interactions between substrates Mg:CTP and Neu5Ac. The structure reported here clearly shows CTP with two $Ca^{2+}$ ions binding in the active site of monomer A with the conformation of the triphosphate moiety pointing in a similar direction to Conformation I in the previously published CDP structure[21] (Figure 2). Our CTP-bound structure also reveals that monomer B binds a CTP molecule without calcium ligands, resulting in a slightly different conformation for the triphosphate moiety. This difference highlights the effect of divalent cations in the positioning of CTP (~~Supplemental~~ Figure S2). However, the electron density for the β and γ phosphates is weak suggesting partial CTP hydrolysis in the B subunit. Nevertheless, for the A subunit, two calcium ions are observed to bind to the CTP triphosphate (Figure 2). The triphosphate group wraps around $Ca^{2+}$(B), allowing the β-phosphate to form a hydrogen bond with Ser15 and the β and γ phosphate to interact with Arg12 of the P-loop. This triphosphate conformation binding to $Ca^{2+}$(B) exposes the backside of the α-phosphate to solvent or a potential sialic acid that would bind in the active site. However, in the absence of $Ca^{2+}$ in the B subunit, the triphosphate group adopts a staggered conformation with no

interaction between the β-phosphate and Ser15 or Arg12. As a result, the side of the α-phosphate, which should be exposed, is pointed back toward the ribose moiety and is less accessible to a nucleophilic attack. Unless otherwise noted, all further discussion of the NmCSS:CTP structure refers strictly to the CTP:$Ca^{2+}$:$Ca^{2+}$ complex, focusing on the A subunit.

Binding of CTP:$Ca^{2+}$:$Ca^{2+}$ stabilizes the P-loop, as evidenced by its lower average B-value (18.9 $Å^2$) and clear electron density as compared to that of the ligand-free structure, including defining the conformation of Lys16. The highly conserved, positively-charged P-loop residues Arg12 and Lys21 (~~Supplemental~~ Figure S1) ion-pair with the negatively charged triphosphate group of CTP (Figure 2). Electrostatic interactions are present between Lys21 and the α-phosphate group as well as between Arg12 and the β- and γ-phosphates. Ser15 hydrogen-bonds with the β-phosphate, and the backbone amino groups of both Lys16 and Gly17 fix the proper positioning of the γ-phosphate through hydrogen-bonding interactions (Figure 2). The amide group of Asn22 in the P-loop makes two hydrogen bonds to the 2'- and 3'-OH of the ribose sugar.

The CTP:$Ca^{2+}$:$Ca^{2+}$ binding pocket P-loop is also stabilized by an interaction between conserved Lys16 and conserved Asp78, which in turn interacts with Arg12 (Figure 2). This interaction helps to position the loop (residues 71–80) that binds to and selects for cytidine base of the nucleotide, where Arg71 donates two hydrogen bonds to O2 and N3 of cytidine, and the main chain carbonyl of Ala80 accepts a hydrogen bond from N4 (Figure 2).

The two calcium ions in the NmCSS:CTP structure—denoted $Ca^{2+}$(A) and $Ca^{2+}$(B)—each play different but important roles in the chemistry of binding and catalysis. $Ca^{2+}$(B) interacts more directly with the triphosphate group, binding to all three phosphates in pentagonal bipyramidal primary coordination sphere. Meanwhile, $Ca^{2+}$(A) coordinates only the α-phosphate directly.

Conserved Asp209 and Asp211, of the DXD sequence, position $Ca^{2+}$(A) through both direct coordination (Asp211) and indirect coordination (Asp209) via $Ca^{2+}$(A)-bound waters. (Figure 2) This finding supports previous activity studies of the poorly-functioning D209A and D211A NmCSS mutants [25]. These studies showed that, while the D209A and D211A mutations are both detrimental to enzyme function, increased concentrations of $Mg^{2+}$ increases the reaction rate of D211A two times more than it increases the reaction rate for D209A. This is consistent with the structure that demonstrates Asp211 directly coordinates the divalent metal ion, but Asp209 interacts with the metal ion water ligands. Sequence conservation also suggests ~~the~~ a less ~~essential~~ direct role for Asp209, because it is a glutamate in some species, including *Drosophila* (Supplemental Figure 1).

Divalent cations are strictly required for catalytic activity.[4, 25] While the majority of CSS enzymes require $Mg^{2+}$ or $Mn^{2+}$, most are either inhibited or display greatly diminished activity with $Ca^{2+}$.[4] We also confirmed that $Ca^{2+}$ inhibits NmCSS with an $IC_{50}$ value of 8.8 ± 0.4 mM (Figure S3). However, given that $Ca^{2+}$ coordination is very similar to $Mg^{2+}$ coordination geometries, this CTP:$Ca^{2+}$:$Ca^{2+}$ complex structure reported here is an ideal Michaelis complex analog of the first substrate binding in this ordered Bi-Bi catalytic mechanism. Furthermore, the CTP-$Ca^{2+}$(B) substrate complex here is very similar to the CTP-$Mg^{2+}$ complex observed in *E. coli* CMP-Kdo synthetase,[23] where the $Mg^{2+}$ ion is coordinated by all three phosphates of CTP. Unfortunately, this CMP-Kdo synthetase structure did not observe the second $Mg^{2+}$ ion binding site but speculated it would bind in similar location to the $Ca^{2+}$(A) ion reported here.[23] However, a $Mg^{2+}$ ion was observed in another CMP-Kdo synthetase structure in a similar location to the $Ca^{2+}$(A) ion.[24]

***Binding of sialic acid induces active site closing***

Conformational changes are seen in the active site of *E. coli* CMP-Kdo-forming enzyme upon binding of an analog of 2-keto-3-deoxymanno-octulonic acid (Kdo),[23, 24] leading us to hypothesize a similar closed conformation my occur in NmCSS. To successfully capture this state, 2-deoxy-2,3-~~di~~dehydro-*N*-acetylneuraminic acid (Neu5Ac2en) was utilized. Neu5Ac2en is a dehydrated sialic acid analog that lacks the attacking C2-OH group responsible for formation of CMP-sialic acid and having instead a double bond between C2 and C3. In the absence of this hydroxyl group, Neu5Ac2en can bind in the active site pocket with CTP, but traps the enzyme in an intermediate state that parallels the enzyme structural state before catalysis occurs. Inhibition studies confirmed that Neu5Ac2en was an inhibitor with an $IC_{50}$ value of 0.13 ± 0.01 mM under the assay conditions used (Figure S4).

Neu5Ac2en was successfully trapped in the NmCSS active site; however, the structure revealed that during crystallization, the enzyme hydrolyzed CTP to CMP, and CMP was observed bound in the active site with bound Neu5Ac2en (Figure 1B). Nevertheless, the crystal structure of this ternary complex revealed the enzyme in a more closed state, relative to ligand-free and Ca:CTP bound structures (Figure 1B and Figure 3).

The closed state of NmCSS:CMP:Neu5Ac2en is brought about by rotation about pivot points located at the termini of β-strands 5 and 8 at the base of the dimerization domain. The flexible nature of the residues at this location at the boundary of the nucleotide-binding and dimerization domain, including conserved Ser132, Ala133, and Gly176, enables active site closure without enacting large conformational change in the individual domains. The nucleotide-binding domain (residues 1–134 and 175–224) of the CTP-bound and the CMP:Neu5Ac2en-bound conformations superimpose with an RMSD of only 0.430 Å for all modeled equivalent alpha carbons. At the same

time, the dimerization domain (residues 135–174) of the CTP-bound and the CMP:Neu5Ac2en-bound conformations superimpose with an RMSD of only 0.658 Å for all modeled equivalent alpha carbons. While the domains themselves remain rigid, the angle between them changes significantly, moving NmCSS into the closed conformation resulting in the dimerization domain of one subunit closing in on the active site of the other subunit in the dimer. In the CMP:Neu5Ac2en-bound structure, the dimerization domain has rotated so that the β5/β6 loop and $3_{10}$ helix cover most of the exposed surface of the occupied active site, closing off the active site from bulk solvent (Figure 3).

Active site closing is initiated through interactions between the sialic acid analogue and the dimerization domain of the other monomer, monomer B (Figure 3B and Figures 4A and 4B). Lys142 of monomer B, located at the end of the dimerization domain's $3_{10}$ helix, and the backbone nitrogen of Arg165, reach into the active site of monomer A to interact with Neu5Ac2en's carboxylate group. Lys142 and the Leu161 backbone carbonyl each form a hydrogen bond with the C7-OH. The Glu162 backbone carbonyl oxygen hydrogen-bonds with C4-OH. After initial closing, which involved interactions between protein and sialic acid, the closed conformation is stabilized by several inter-monomer interactions. Gln166(B) of the $3_{10}$ helix bridges the gap between monomers through hydrogen bonding with the backbone carbonyl of Asp78(A) (Figure 3B). His138(B) and Arg173(A) interact via π-π-stacking and His138(B) also forms a salt bridge with Asp209(A).

In addition to the interactions with the dimerization domain of the opposite monomer, sialic acid also interacts with several highly or partially conserved residues (~~Supplemental~~ Figure S1) in the nucleotide binding domain. The methyl group in the *N*-acetyl ~~methyl group~~ of Neu5Ac2en lies in a hydrophobic pocket made up of Leu102, Tyr179, and Phe192. Additionally, The Nε2 of

Gln104 hydrogen-bonds with O8 of Neu5Ac2en. The Ser82 backbone nitrogen hydrogen-bonds to O4 of Neu5Ac2en while its Oγ hydrogen-bonds with the *N*-acetyl nitrogen (Figure 4A and 4B).

In spite of having $Mg^{2+}$ present in crystallization solution, no cations are observed in the active site of the NmCSS:CMP:Neu5Ac2en structure. This is most likely due to the absence of the cytidine nucleotide's β- and γ- phosphates, which were hydrolyzed during the course of the crystallography experiment.

***Enzyme activation by citrate?***

Unaccountable electron density was observed at the dimer interface in the NmCSS:CMP:Neu5Ac2en structure. Given the crystals were grown in the presence of citrate (100 mM), a citrate molecule was modeled in which fits the electron density acceptably (~~Supplemental~~ Figure S~~3a~~5A). This citrate molecule bridges the gap between the two dimerization domains and also forms a conduit between the one dimerization domain and the nucleotide binding domain of the opposite monomer (~~Supplemental~~ Figure ~~3A~~S5A). Citrate's two terminal carboxylate groups reach across the space between the two monomers at their β5/β6 loop, hydrogen-bonding with the backbone nitrogens of the Glu137 in each. The citrate also connects two side chains from opposite monomers, the central carboxylate interacting with the Nδ1 of His138 and the one of the terminal carboxylates interacting with the Nε2 of His204.

Considering the importance of the β5/β6 loop in enzyme closing and the role of His138 in stabilizing the NmCSS closed conformation, we hypothesized that citrate may affect CSS activity. Indeed, after adding citrate to the reaction buffer, the production of CMP-sialic acid was increased moderately (~~Supplemental~~ Figure S~~3B~~5B). Further work will be necessary to determine the precise role of citrate in the regulation of CSS activity.

***Structure with CMP-Neu5Ac product bound***

The crystal structure of NmCSS with CMP-Neu5Ac product bound revealed a structure in the open state conformation similar to the ligand-free and Ca-CTP bound state of NmCSS. This suggests that after binding CTP and Neu5Ac, product formation drives the re-opening of the active site, possibly to release products. Sialic acid interactions with the nucleotide-binding domain are maintained, but as a new bond is formed between the sialic acid and the α-phosphate, the sugar group moves deeper into the active site pocket of the nucleotide binding domain breaking interactions between the sugar and dimerization domain, and NmCSS transitions back into an open state. At this point, $Ca^{2+}$(B) leaves the active site with the pyrophosphate, but $Ca^{2+}$(A) remains, coordinating the Neu5Ac carboxylate group, an oxygen in the phosphate moiety of CMP-Neu5Ac, and four ordered water molecules in an octahedral geometry (Figure 5**)**. The ordered waters are also held in place with the help of the metal-binding DXD motif of Asp209 and Asp211. The DXD-containing loop is nudged open a small amount so Asp211 no longer coordinates $Ca^{2+}$(A) directly as observed in the Ca-CTP bound structure.

***Comparison with other structures***

With less than 30% sequence identity to NmCSS, the crystal structures of *E. coli* CMP-Kdo synthetases KdsB[23] and KpsU[24] as well as mouse CSS (MmCSS)[22] have parallels as well as differences with the structures presented here. Although several residues are highly conserved (~~Supplemental~~ Figure S1), the process and means of closed state formation varies from species to species.

While the *E. coli* CMP-Kdo synthetases are active dimers, they do not possess dimerization domains that entwine and lock the two monomers together as observed in NmCSS. This flatter dimerization interface only buries 2673 Å$^2$ of surface area of both monomers in the closed state

compared to NmCSS closed state, which buries 4460 Å$^2$. However, the *E. coli* structures also display a conformational change that closes the active site pocket in the presence of two substrates, but not after product formation, reminiscent of what we observe in NmCSS.

While we were unable to capture the NmCSS:CTP:sialic acid structure, the KdsB:CTP: 2-keto-2β,3-~~di~~deoxymanno-octulonic acid (Kdo2en~~2β-deoxy-Kdo~~) structure indicates that the guanidinium group of Arg164 (Arg165 in NmCSS) is involved in CTP γ-phosphate interaction (Figures 6A and B). Superposition of the NmCSS:CTP and NmCSS:CMP:Neu5Ac2en structures suggests a similar function for Arg165 in NmCSS (Figure 6A). Because the *E. coli* CMP-Kdo synthetases form different dimerization interactions and lack the dimerization domain, no residues of one monomer contact the sugar bound in the active site of the partner monomer. However, Glu210 of the nucleotide binding domain of KdsB hydrogen bonds with C4-OH of the Kdo analog through its carboxylate group and backbone nitrogen (Figure 6B). Structurally, KdsB Glu210 is in the same position as Glu162 of NmCSS; however, in KdsB, Glu210 is from the same monomer as the active site in which Kdo2en ~~2β-deoxy-Kdo~~ is situated, but in NmCSS Glu162 is from the dimerization domain of the opposite monomer. KdsB Arg157, which ion-pairs with Kdo2en ~~2β-deoxy-Kdo~~ carboxylate group in a position similar to that of CSS Lys142, is also from the same monomer.

The dimerization domain of mouse CSS, which is similar to NmCSS, does interact with the sugar in the opposite monomer's active site through two arginine residues. Similar to Arg165 of NmCSS, the Arg202 backbone amino group of MmCSS binds to the Neu5Ac carboxylate group. Interestingly, in MmCSS the arginine guanidinium group ion-pairs with the Neu5Ac carboxylate group as well, giving the Arg202 side chain a role in closed-state stabilization. The R202A mutation has been shown to be detrimental but not fatal to enzyme activity, while the NmCSS

R165A mutation results in a complete loss of activity [36]. The ability of MmCSS to function without Arg202 may be due to additional closed-state stabilization from MmCSS Arg199, which hydrogen bonds with both the Neu5Ac C7 hydroxyl and the *N*-acetyl carbonyl group (Figure 6C). The position of Arg199 allows it to also form three new interactions with Glu211 and Gln229 of the partner monomer (Figure 6C). Due to this extra closed-state stabilization, MmCSS remains closed even after product formation. NmCSS Arg165, however, may play a different role in directing NmCSS enzyme-substrate conformation, as we discuss below.

***Modeling of CSS:CTP:$Ca^{2+}$:$Ca^{2+}$:Neu5Ac***

Arg165 is strictly conserved in both CMP-sialic acid and CMP-Kdo synthetases (~~Supplemental~~ Figure S1), yet there are no explicit interactions between Arg165 side chain atoms and Neu5Ac2en or CMP in the NmCSS:CMP:Neu5Ac2en structure. A superposition of CTP from the NmCSS:CTP structure onto the NmCSS:CMP:Neu5Ac2en structure indicates that Arg165(B) could form electrostatic interactions with the γ-phosphate of CTP (Figure 6A), which would corroborate with the function of its equivalent residue in KdsB. The side chain electron density for Arg165 in NmCSS:CMP:Neu5Ac2en is weak and the position shown in Figure 6A would not be possible in the presence of $Ca^{2+}$(A). However, since the structure is missing the complete triphosphate moiety, it cannot be regarded as a true intermediate state of the NmCSS catalytic cycle. An alternative Arg165 rotamer has been modeled which maintains the ion pair between Arg165 and the γ-phosphate, but does not clash with $Ca^{2+}$(A) (Figure 7A).

Since Arg165 is a long, positively charged residue capable of reaching across the gap between the dimerization and nucleotide binding domains, the highly conserved nature of Arg165 may be due to the need for proper positioning of the backbone of residue 165. Perhaps the anchoring of

Arg165 with the γ-phosphate is necessary in order to allow its backbone amino group to interact with the Neu5Ac carboxylate group.

***Activity of NmCSS mutants.***

The four crystal structures presented above led us to hypothesize the functional role of two key residues in helping to stabilize the closing of the active site, making them important in the catalytic mechanism proposed below. Specifically, it appears that Glu162 and Arg165 may play an important role by reaching across the dimer interface to possibly interact with substrates in the other monomer's active site. Glu162 and Arg165 interact with the sialic acid and the triphosphate moiety from CTP, respectively, in the other subunit's active site (Figure 3B). Glu162 also stabilizes the active-site closure by hydrogen bonding with the mainchain nitrogen of Phe192 in the other monomer.

Indeed, the E162A and E162Q mutants displayed six-fold lower activity than the wild-type NmCSS, while the R165A mutant was approximately six hundred-fold less active than wild-type (Table 2). These results suggest that the active-site closure, stabilized by cross-monomer interactions involving residues Glu162 and Arg165, is necessary for efficient catalysis.

## DISCUSSION

### *Basis for substrate tolerance*

In the chemoenzymatic synthesis of complex carbohydrates, NmCSS has proven itself to be a very useful enzyme, activating several forms of sialic acids as diverse as 2-keto-3-deoxy-D-manno-octulosonic acid (Kdo) and *N*-azidoacetylneuraminic acid ($Neu5AcN_3$). The structures presented here enable us to better understand the basis of this tolerance. First off, the flexible nature of the Lys142 side chain would likely allow for substitutions at O7 as well as small changes in the

position of the Neu5Ac carboxylate group. Additionally, analysis of the active site pocket after closing suggests that a solvent pocket near C7, C8, and C9 provides space for bulky modifications to O9 (Figure 4A). It could also provide space for sialic acid to shift deeper into the active site pocket in order to allow *N*-acetyl modification as well. In fact, these are the modifications that are tolerated by the enzyme.[7, 12, 19] Modification of the C8 hydroxyl group, however, results in a drastic decrease in activity.[12] In light of the structures presented here, this is likely due to the importance of the Gln104–O8 interaction in the initial docking of sialic acid.

Although few crystal structures of NmCSS have been available previously, several groups have successfully created mutants of NmCSS with increased or modified substrate specificity. The S81R mutant of NmCSS, for example, has been shown to better tolerate O8-methyl substitutions.[26] Model-guided mutagenesis has also created mutants that have more general tolerance for *N*-acyl-modified sialic acids [26]. Despite these success stories however, there is still a need for mutants that can accept substrates with more than one modification such as Neu5Gc8OMe or Kdo8OMe. Based on the NmCSS:CMP:Neu5Ac2en and NmCSS:CMP-Neu5Ac structures presented here, shortening or mutating the loop between β-sheet 8 and 9 may allow more room for C8 modifications as well as provide more space for small shifts of sialic acid due to multiple modifications..

***Role of $Mg^{2+}$ in catalysis***

Previous studies have suggested that only $Mg^{2+}$ can be used by NmCSS to catalyze nucleotide transfer to sialic acid [28]. Since product was formed over a month's time in the crystallization drop with $Ca^{2+}$ rather than $Mg^{2+}$, clearly the identity of the cation is not strictly limited to $Mg^{2+}$, but catalysis using $Ca^{2+}$ may be much slower than with $Mg^{2+}$. In fact, calcium has been reported to substitute for $Mg^{2+}$ in other CSS enzymes, although usually with less catalytic efficiency.[37-39]

Figure 2 and ~~Supplemental~~ Figure S2 demonstrate the important role of divalent cations in proper positioning of the triphosphate groups. Divalent metal $M^{2+}$(B) coordinates all three phosphate groups and orients the scissile bond between the α-phosphate and β-phosphate to be along the same axis as the attack by Neu5Ac on the α-phosphate. $M^{2+}$(B) also increases the leaving group potential of the pyrophosphate moiety by stabilizing its negative charge. Even with proper orientation and the presence of a good leaving group, however, the C2-OH of Neu5Ac must first be deprotonated before it can attack the α-phosphate, and there is no basic residue within close enough proximity to play this role. $M^{2+}$(A) likely solves this problem by decreasing the *p*Ka of the hydroxyl group by ligating directly to the $M^{2+}$(A) ion. We propose that both the anomeric C2-OH and the C1-carboxylate group of Neu5Ac directly ligate to $M^{2+}$(A), which positions the anomeric C2 hydroxyl group in prime position for a nucleophilic attack on the α-phosphate. This model is corroborated by the NmCSS:CMP-Neu5Ac structure that has the Neu5Ac carboxylate group ligated to $Ca^{2+}$(A) after catalysis. Hydroxyl activation via $Mg^{2+}$ coordination has also been proposed for the catalysis of KdsB,[23] which uses the metal to activate 2-keto-3-deoxymanno-octulonic acid (Kdo). Based on structural analysis and EPR data,[23, 27] the locations of the $Mg^{2+}$ in both EcKdsB and AaKdsB have been elucidated. Overlay of AaKdsB with the NmCSS:CTP:Ca:Ca structure shows that the metal positions in these structures are similar, supporting a similar mechanism as well.

***Proposed catalytic cycle for NmCSS***

Careful analysis of each structure presented here allows us to hypothesize an enzyme conformation for each step in the catalytic cycle of NmCSS catalysis (Figure 7B). At the start of the catalytic cycle, CTP binds in the active site pocket along with $M^{2+}$(A) and $M^{2+}$(B), which properly position the phosphate groups for catalysis and allow space for Neu5Ac to enter the active site pocket. Arg12 moves to interact with the β- and γ-phosphates. With CTP in this position,

Neu5Ac loosely binds in the available space in the active site of monomer A, with its carboxylate group and the anomeric carbon hydroxyl group in the coordination shell of $M^{2+}$(A). The binding of Neu5Ac initiates active site closure as the interactions between sialic acid and Lys142, Leu161, Glu162, and Arg165 pull sialic acid, CTP, and the nucleotide ~~bind~~ binding domain toward the dimerization domain (Figure 3). Once initiated, the closed state is stabilized by Arg165 ion pairing with the γ-phosphate and several inter-monomer interactions. As the dimerization domain comes near to Neu5Ac, coordination to $M^{2+}$(A) allows Neu5Ac-C2-OH to be deprotonated, with the proton possibly being shuttled through water ligands to Asp209. The restricted movement by the presence of the dimerization domain forces the deprotonated oxygen toward CTP's α-phosphate, which has an increased electrophilic nature due to the two $M^{2+}$'s that coordinate the triphosphate group and the Arg165 to γ-phosphate ion pair. As the bond between the α-phosphate and β-phosphate breaks and the new bond between Neu5Ac-O2 and α-phosphate forms, the α-phosphate passes through a trigonal bipyramidal transition state, and pyrophosphate and its associated $M^{2+}$(B) leave the active site. Once product has been formed, the sugar is more closely associated with the nucleotide-binding domain and can no longer maintain its hydrogen bonding and electrostatic interactions with the dimerization domain, so NmCSS:CMP-Neu5Ac reverts back to the open state. The product diffuses from the active site and the cycle can begin again.

Although NmCSS has been used in chemoenzymatic synthesis of sialic acid-containing structures for over a decade, the causes for its broad substrate tolerance and the role of divalent cations in catalysis has finally been shown through the four structures presented here. This work describes how sugar interaction with both monomers of the NmCSS homodimer are responsible for active site closure and the role of divalent cations in the transfer of CMP to sialic acid, laying the groundwork for future structure-guided enzyme engineering.

## ACCESSION CODES

The atomic coordinates and structure factors (codes 6CKJ, 6CKK, 6CKL, and 6CKM) have been deposited in the Protein Data Bank (https://www.rcsb.org).

Uniprot Accession ID of N-acylneuraminate cytidylyltransferase: P0A0Z8

## Author Contributions

M.M.M., Y.L., H.Y., J.B.M., and A.J.F. performed experiments. All authors analyzed data and wrote the paper. All authors have read and approved the final version of the manuscript.

## Funding

This work was partially supported by the United States National Institutes of Health (NIH) grants U01GM120419, U01GM125288, and R01AI130684. The content is solely the responsibility of the authors and does not necessarily represent the official views of the National Institutes of Health.

## Notes

The authors declare no completing financial interest with the contents of this article.

## ACKNOWLEDGMENTS

This work is based upon research conducted at the Northeastern Collaborative Access Team beamlines, which are funded by the National Institute of General Medical Sciences from the National Institutes of Health (P30 GM124165). The Pilatus 6 M detector on 24-ID-C beam line is funded by a NIH-ORIP HEI grant (S10 RR029205). This research used resources of the Advanced Photon Source, a U.S. Department of Energy (DOE) Office of Science User Facility operated for the DOE Office of Science by Argonne National Laboratory under Contract No. DE-AC02-06CH11357. Use of the Stanford Synchrotron Radiation Lightsource, SLAC National Accelerator

Laboratory, is supported by the U.S. Department of Energy, Office of Science, Office of Basic Energy Sciences under Contract No. DE-AC02-76SF00515. The SSRL Structural Molecular Biology Program is supported by the DOE Office of Biological and Environmental Research, and by the National Institutes of Health, National Institute of General Medical Sciences (including P41GM103393). The contents of this publication are solely the responsibility of the authors and do not necessarily represent the official views of NIGMS or NIH.

## REFERENCES


[1] Varki, A. (2008) Sialic acids in human health and disease, *Trends Mol Med 14*, 351-360.

[2] Li, Y., and Chen, X. (2012) Sialic acid metabolism and sialyltransferases: natural functions and applications, *Appl Microbiol Biotechnol 94*, 887-905.

[3] Sellmeier, M., Weinhold, B., and Munster-Kuhnel, A. (2015) CMP-Sialic Acid Synthetase: The Point of Constriction in the Sialylation Pathway, *Top Curr Chem 366*, 139-167.

[4] Mizanur, R. M., and Pohl, N. L. (2008) Bacterial CMP-sialic acid synthetases: production, properties, and applications, *Appl Microbiol Biotechnol 80*, 757-765.

[5] Chen, X., and Varki, A. (2010) Advances in the biology and chemistry of sialic acids, *ACS Chem Biol 5*, 163-176.

[6] Li, W., McArthur, J. B., and Chen, X. (2019) Strategies for chemoenzymatic synthesis of carbohydrates, *Carbohydr Res 472*, 86-97.

[7] Yu, H., Yu, H., Karpel, R., and Chen, X. (2004) Chemoenzymatic synthesis of CMP-sialic acid derivatives by a one-pot two-enzyme system: comparison of substrate flexibility of three microbial CMP-sialic acid synthetases, *Bioorg Med Chem 12*, 6427-6435.

[8] Chokhawala, H. A., Yu, H., and Chen, X. (2007) High-throughput substrate specificity studies of sialidases by using chemoenzymatically synthesized sialoside libraries, *Chembiochem 8*, 194-201.

[9] Yu, H., Huang, S., Chokhawala, H., Sun, M., Zheng, H., and Chen, X. (2006) Highly efficient chemoenzymatic synthesis of naturally occurring and non-natural alpha-2,6-linked sialosides: a P. damsela alpha-2,6-sialyltransferase with extremely flexible donor-substrate specificity, *Angew Chem Int Ed Engl 45*, 3938-3944.

[10] Yu, H., Chokhawala, H., Karpel, R., Yu, H., Wu, B., Zhang, J., Zhang, Y., Jia, Q., and Chen, X. (2005) A multifunctional Pasteurella multocida sialyltransferase: a powerful tool for the synthesis of sialoside libraries, *J Am Chem Soc 127*, 17618-17619.

[11] Yu, H., Cheng, J., Ding, L., Khedri, Z., Chen, Y., Chin, S., Lau, K., Tiwari, V. K., and Chen, X. (2009) Chemoenzymatic synthesis of GD3 oligosaccharides and other disialyl glycans containing natural and non-natural sialic acids, *J Am Chem Soc 131*, 18467-18477.

[12] Li, Y., Yu, H., Cao, H., Muthana, S., and Chen, X. (2012) Pasteurella multocida CMP-sialic acid synthetase and mutants of Neisseria meningitidis CMP-sialic acid synthetase with improved substrate promiscuity, *Appl Microbiol Biotechnol 93*, 2411-2423.

[13] Liu, G., Jin, C., and Jin, C. (2004) CMP-N-acetylneuraminic acid synthetase from Escherichia coli K1 is a bifunctional enzyme: identification of minimal catalytic domain for synthetase activity and novel functional domain for platelet-activating factor acetylhydrolase activity, *J Biol Chem 279*, 17738-17749.

[14] Yu, H., Ryan, W., Yu, H., and Chen, X. (2006) Characterization of a bifunctional cytidine 5'-monophosphate N-acetylneuraminic acid synthetase cloned from Streptococcus agalactiae, *Biotechnol Lett 28*, 107-113.

[15] Mizanur, R. M., and Pohl, N. L. (2007) Cloning and characterization of a heat-stable CMP-N-acylneuraminic acid synthetase from Clostridium thermocellum, *Appl Microbiol Biotechnol 76*, 827-834.

[16] Yu, H., Santra, A., Li, Y., McArthur, J. B., Ghosh, T., Yang, X., Wang, P. G., and Chen, X. (2018) Streamlined chemoenzymatic total synthesis of prioritized ganglioside cancer antigens, *Org Biomol Chem 16*, 4076-4080.

[17] Yu, H., Yan, X., Autran, C. A., Li, Y., Etzold, S., Latasiewicz, J., Robertson, B. M., Li, J., Bode, L., and Chen, X. (2017) Enzymatic and Chemoenzymatic Syntheses of Disialyl Glycans and Their Necrotizing Enterocolitis Preventing Effects, *J Org Chem 82*, 13152-13160.

[18] Khedri, Z., Li, Y., Muthana, S., Muthana, M. M., Hsiao, C. W., Yu, H., and Chen, X. (2014) Chemoenzymatic synthesis of sialosides containing C7-modified sialic acids and their application in sialidase substrate specificity studies, *Carbohydr Res 389*, 100-111.

[19] He, N., Yi, D., and Fessner, W. D. (2011) Flexibility of Substrate Binding of Cytosine-5 '-Monophosphate-N-Acetylneuraminate Synthetase (CMP-Sialate Synthetase) from Neisseria meningitidis: An Enabling Catalyst for the Synthesis of Neo-sialoconjugates, *Advanced Synthesis & Catalysis 353*, 2384-2398.

[20] Yu, H., Cao, H., Tiwari, V. K., Li, Y., and Chen, X. (2011) Chemoenzymatic synthesis of C8-modified sialic acids and related alpha2-3- and alpha2-6-linked sialosides, *Bioorg Med Chem Lett 21*, 5037-5040.

[21] Mosimann, S. C., Gilbert, M., Dombroswki, D., To, R., Wakarchuk, W., and Strynadka, N. C. (2001) Structure of a sialic acid-activating synthetase, CMP-acylneuraminate synthetase in the presence and absence of CDP, *J Biol Chem 276*, 8190-8196.

[22] Krapp, S., Munster-Kuhnel, A. K., Kaiser, J. T., Huber, R., Tiralongo, J., Gerardy-Schahn, R., and Jacob, U. (2003) The crystal structure of murine CMP-5-N-acetylneuraminic acid synthetase, *J Mol Biol 334*, 625-637.

[23] Heyes, D. J., Levy, C., Lafite, P., Roberts, I. S., Goldrick, M., Stachulski, A. V., Rossington, S. B., Stanford, D., Rigby, S. E., Scrutton, N. S., and Leys, D. (2009) Structure-based mechanism of CMP-2-keto-3-deoxymanno-octulonic acid synthetase: convergent evolution of a sugar-activating enzyme with DNA/RNA polymerases, *J Biol Chem 284*, 35514-35523.

[24] Jelakovic, S., and Schulz, G. E. (2001) The structure of CMP:2-keto-3-deoxy-manno-octonic acid synthetase and of its complexes with substrates and substrate analogs, *J Mol Biol 312*, 143-155.

[25] Horsfall, L. E., Nelson, A., and Berry, A. (2010) Identification and characterization of important residues in the catalytic mechanism of CMP-Neu5Ac synthetase from Neisseria meningitidis, *FEBS J 277*, 2779-2790.

[26] Yi, D., He, N., Kickstein, M., Metzner, J., Weiss, M., Berry, A., and Fessner, W. D. (2013) Engineering of a Cytidine 5 '-Monophosphate-Sialic Acid Synthetase for Improved Tolerance to Functional Sialic Acids, *Advanced Synthesis & Catalysis 355*, 3597-3612.

[27] Schmidt, H., Mesters, J. R., Wu, J., Woodard, R. W., Hilgenfeld, R., and Mamat, U. (2011) Evidence for a two-metal-ion mechanism in the cytidyltransferase KdsB, an enzyme involved in lipopolysaccharide biosynthesis, *PLoS One 6*, e23231.

[28] Blacklow, R. S., and Warren, L. (1962) Biosynthesis of sialic acids by Neisseria meningitidis, *J Biol Chem 237*, 3520-3526.

[29] Andreini, C., Cavallaro, G., Lorenzini, S., and Rosato, A. (2013) MetalPDB: a database of metal sites in biological macromolecular structures, *Nucleic Acids Res 41*, D312-319.

[30] Zheng, H., Cooper, D. R., Porebski, P. J., Shabalin, I. G., Handing, K. B., and Minor, W. (2017) CheckMyMetal: a macromolecular metal-binding validation tool, *Acta Crystallogr D Struct Biol 73*, 223-233.

[31] Kabsch, W. (2010) Xds, *Acta Crystallogr D Biol Crystallogr 66*, 125-132.

[32] Evans, P. R., and Murshudov, G. N. (2013) How good are my data and what is the resolution?, *Acta Crystallogr D Biol Crystallogr 69*, 1204-1214.
[33] McCoy, A. J., Grosse-Kunstleve, R. W., Adams, P. D., Winn, M. D., Storoni, L. C., and Read, R. J. (2007) Phaser crystallographic software, *J Appl Crystallogr 40*, 658-674.
[34] Murshudov, G. N., Skubak, P., Lebedev, A. A., Pannu, N. S., Steiner, R. A., Nicholls, R. A., Winn, M. D., Long, F., and Vagin, A. A. (2011) REFMAC5 for the refinement of macromolecular crystal structures, *Acta Crystallogr D Biol Crystallogr 67*, 355-367.
[35] Afonine, P. V., Grosse-Kunstleve, R. W., Echols, N., Headd, J. J., Moriarty, N. W., Mustyakimov, M., Terwilliger, T. C., Urzhumtsev, A., Zwart, P. H., and Adams, P. D. (2012) Towards automated crystallographic structure refinement with phenix.refine, *Acta Crystallogr D Biol Crystallogr 68*, 352-367.
[36] Munster, A. K., Weinhold, B., Gotza, B., Muhlenhoff, M., Frosch, M., and Gerardy-Schahn, R. (2002) Nuclear localization signal of murine CMP-Neu5Ac synthetase includes residues required for both nuclear targeting and enzymatic activity, *J Biol Chem 277*, 19688-19696.
[37] Schauer, R., Haverkamp, J., and Ehrlich, K. (1980) Isolation and characterization of acylneuraminate cytidylyltransferase from frog liver, *Hoppe Seylers Z Physiol Chem 361*, 641-648.
[38] Bravo, I. G., Barrallo, S., Ferrero, M. A., Rodriguez-Aparicio, L. B., Martinez-Blanco, H., and Reglero, A. (2001) Kinetic properties of the acylneuraminate cytidylyltransferase from Pasteurella haemolytica A2, *Biochem J 358*, 585-598.
[39] Rodriguez-Aparicio, L. B., Luengo, J. M., Gonzalez-Clemente, C., and Reglero, A. (1992) Purification and characterization of the nuclear cytidine 5'-monophosphate N-acetylneuraminic acid synthetase from rat liver, *J Biol Chem 267*, 9257-9263.

**Table 1. Data Processing and Refinement Statistics.**

| Complex | CSS | CSS:CTP:Ca:Ca | CSS:CMP:Neu5Ac2en | CSS:CMP-Neu5Ac:Ca |
|---|---|---|---|---|
| PDBID | 6CKJ | 6CKK | 6CKL | 6CKM |
| Beamline | APS 24-ID-C | SSRL 7-1 | SSRL 7-1 | SSRL 7-1 |
| Wavelength (Å) | 0.9791 | 1.03316 | 0.97950 | 1.12709 |
| Space Group | C222 | $P2_12_12_1$ | $C222_1$ | C222 |
| Unit Cell Parameters (Å) | a=93.78 b=155.06 c=38.78 | a=43.19 b=69.56 c=158.21 | a=128.48 b=151.01 c=84.90 | a=93.37 b=156.02 c=38.71 |
| Resolution Range (Å) | 38.78-1.75 (1.78-1.75) | 37.91-1.80 (1.84-1.80) | 97.86-2.68 (2.75-2.68) | 80.13-1.54 (1.58-1.54) |
| No. observed reflections | 95,613 (4830) | 142,810 (9562) | 71,705 (4482) | 145,811 (9292) |
| No. unique reflections | 27,855 (1446) | 42,666 (2883) | 22,814 (1615) | 41,624 (2739) |
| Completeness (%) | 96.0 (91.8) | 93.8 (87.7) | 97.1 (94.2) | 98.6 (89.4) |
| I/σ (I) | 14.2 (3.9) | 16.64 (3.56) | 11.57 (2.13) | 11.86 (2.52) |
| $R_{merge}$[a] (%) | 6.2 (51.5) | 4.8 (29.1) | 8.9 (50.3) | 6.1 (44.9) |
| $CC_{1/2}$ | 99.5 (79.4) | 99.8 (92.0) | 99.5 (72.7) | 99.7 (79.8) |
| Monomers per ASU | 1 | 2 | 3 | 1 |
| Matthew's Coefficient ($Å^3$/Da) | 2.75 | 2.32 | 2.68 | 2.75 |
| Solvent Content (%) | 55.27 | 46.93 | 54.06 | 55.28 |
| **Refinement Statistics** | | | | |
| No of reflections (F>0) | 27,840 | 40,429 | 21,689 | 41, 623 |
| $R_{factor}$[b] (%) | 15.71 | 20.19 | 19.44 | 15.28 |
| $R_{free}$[b] (%) | 18.65 | 24.96 | 24.17 | 17.63 |
| RMS bond length (Å) | 0.006 | 0.016 | 0.012 | 0.006 |
| RMS bond angle (°) | 0.751 | 1.728 | 1.598 | 0.763 |
| Coordinate Error (Å) | 0.13 | 0.11 | 0.25 | 0.14 |
| **Ramachandran Plot Statistics**[c] | | | | |
| Favored (%) | 98.21 | 97.09 | 98.06 | 98.65 |
| Allowed (%) | 1.79 | 2.69 | 1.49 | 1.35 |
| Outliers (%) | 0.00 | 0.22 | 0.45 | 0.00 |
| | | | | |
| **No. of atoms (B-factor)** | | | | |
| Protein | 1719 (27.40) | 3497 (21.61) | 5174 (44.04) | 1721 (23.49) |
| Ligand | 0 | 58 (20.88) | 123 (37.68) | 41 (25.49) |
| Metal | 2 (37.48) | 3 (30.45) | 0 | 1 (35.30) |
| Solvent | 256 (35.96) | 680 (33.02) | 140 (38.05) | 309 (35.75) |
| | | | | |

$R_{merge} = [\sum_h\sum_i|\boldsymbol{I}_h - \boldsymbol{I}_{hi}|/\sum_h\sum_i\boldsymbol{I}_{hi}]$ where $\boldsymbol{I}_h$ is the mean of $\boldsymbol{I}_{hi}$ observations of reflection *h*. Numbers in parenthesis represent highest resolution shell.

[b] *R*-Factor and [c] $R_{free} = \sum||F_{obs}| - |F_{calc}|| / \sum|F_{obs}|$ x 100 for 95% of recorded data (*R*-Factor) or 5% data ($R_{free}$)

[c] Ramachandran plot statistics from MolProbity

**Table 2.** Relative specific activity of NmCSS mutants compared to the wild-type NmCSS.

| NmCSS | Relative Specific Activity |
|---|---|
| wild-type | $1.00 \pm 0.04$ |
| E162A | $(1.45 \pm 0.11) \times 10^{-1}$ |
| E162Q | $(1.53 \pm 0.04) \times 10^{-1}$ |
| R165A | $(1.63 \pm 0.09) \times 10^{-3}$ |

Figure 1A

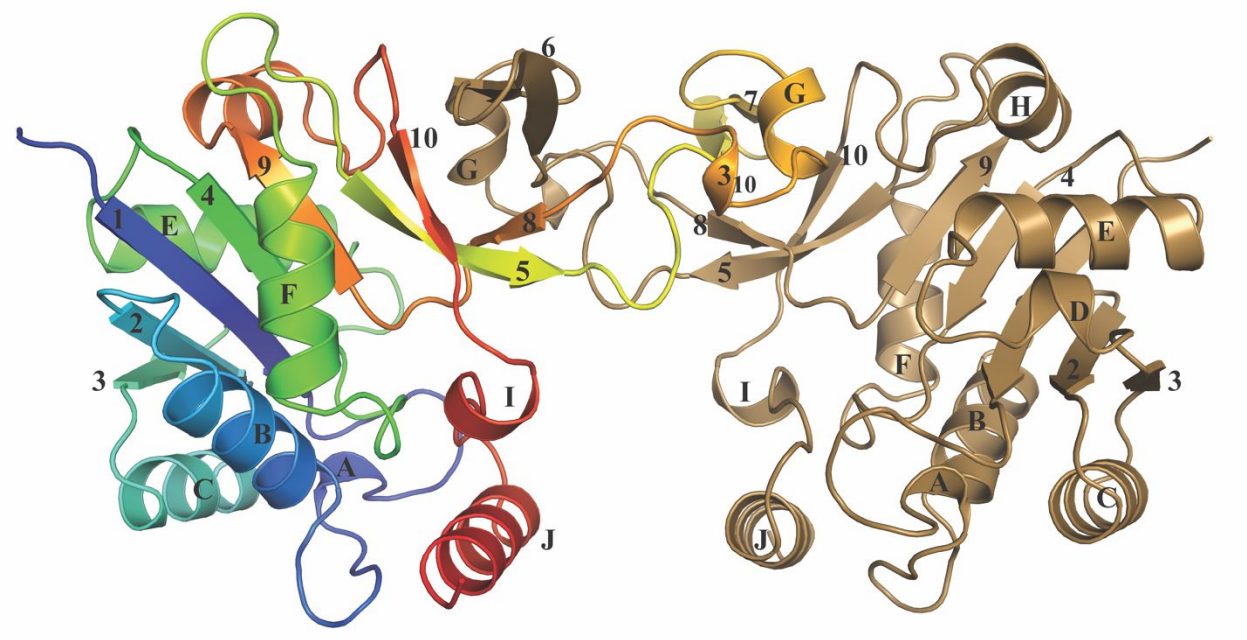


Figure 1B

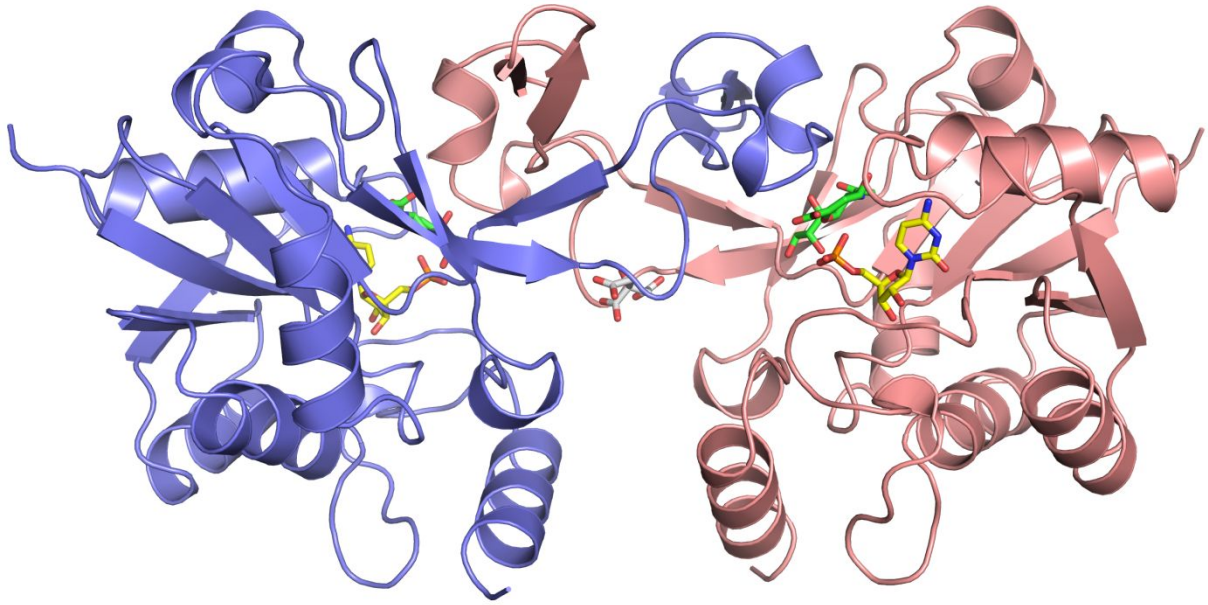

**Figure 1. NmCSS homodimer structure.** (A) Structure of ligand-free NmCSS homodimer. For contrast, one monomer is shown in bronze and the other in the rainbow spectrum starting with blue at the N-terminus and ending with red at the C-terminus. Each monomer consists of a globular

nucleotide-binding domain and an extended dimerization domain where it interacts with its partner monomer. β-Sheets are labeled with numbers and α-helices with letters, with the exception of the $3_{10}$ helix located in the dimerization domain of each monomer. (B) Structure of NmCSS homodimer with ligands CMP and Neu5Ac2en bound in the active site, drawn as sticks with yellow- and green-colored carbon atoms respectively. Citrate binding at dimer interface is drawn in sticks with white-colored carbon atoms.

Figure 2

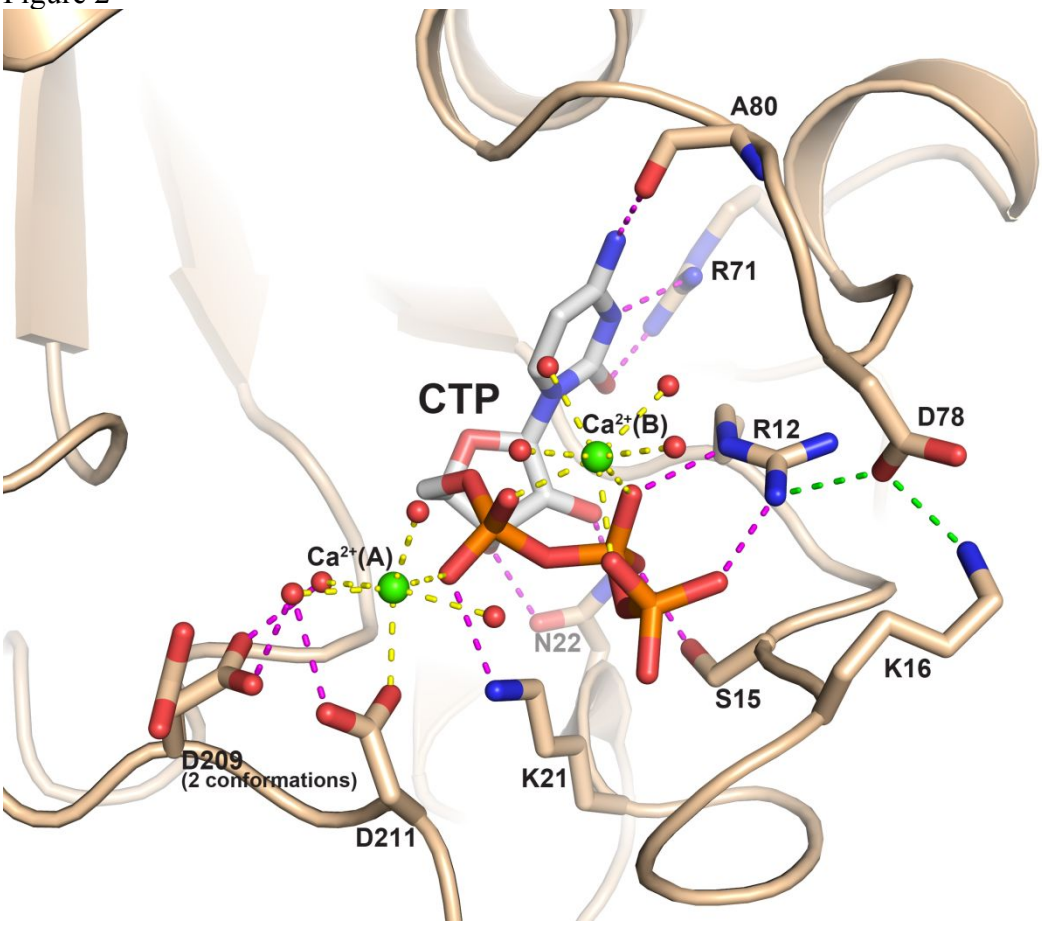


**Figure 2. Binding orientation of CTP in the active site.** CTP (white carbons) bound in the A subunit of the dimer with two calcium ions (green spheres) ligated to the phosphate moieties. Calcium ions (A) and (B) work together with the P-loop (residues 12-22) to properly position and stabilize the negative charge on the triphosphate group. Calcium ion A ligates to the α phosphate, Asp–211, and four water molecules (red spheres). Asp–209, which was observed to adopt two conformations with one binding to the $Ca^{2+}$(A) water ligands, together with Asp211 make up the conserved DXD motif. Calcium ion B ligates to all three phosphates of CTP together with four water molecules. Calcium ligations are highlighted with yellow dashed lines and hydrogen bonds between protein and Ca-CTP are magenta in color, while the P-loop stabilization interaction between Arg12-Asp78-Lys16 is drawn with green dashed lines.

Figure 3A

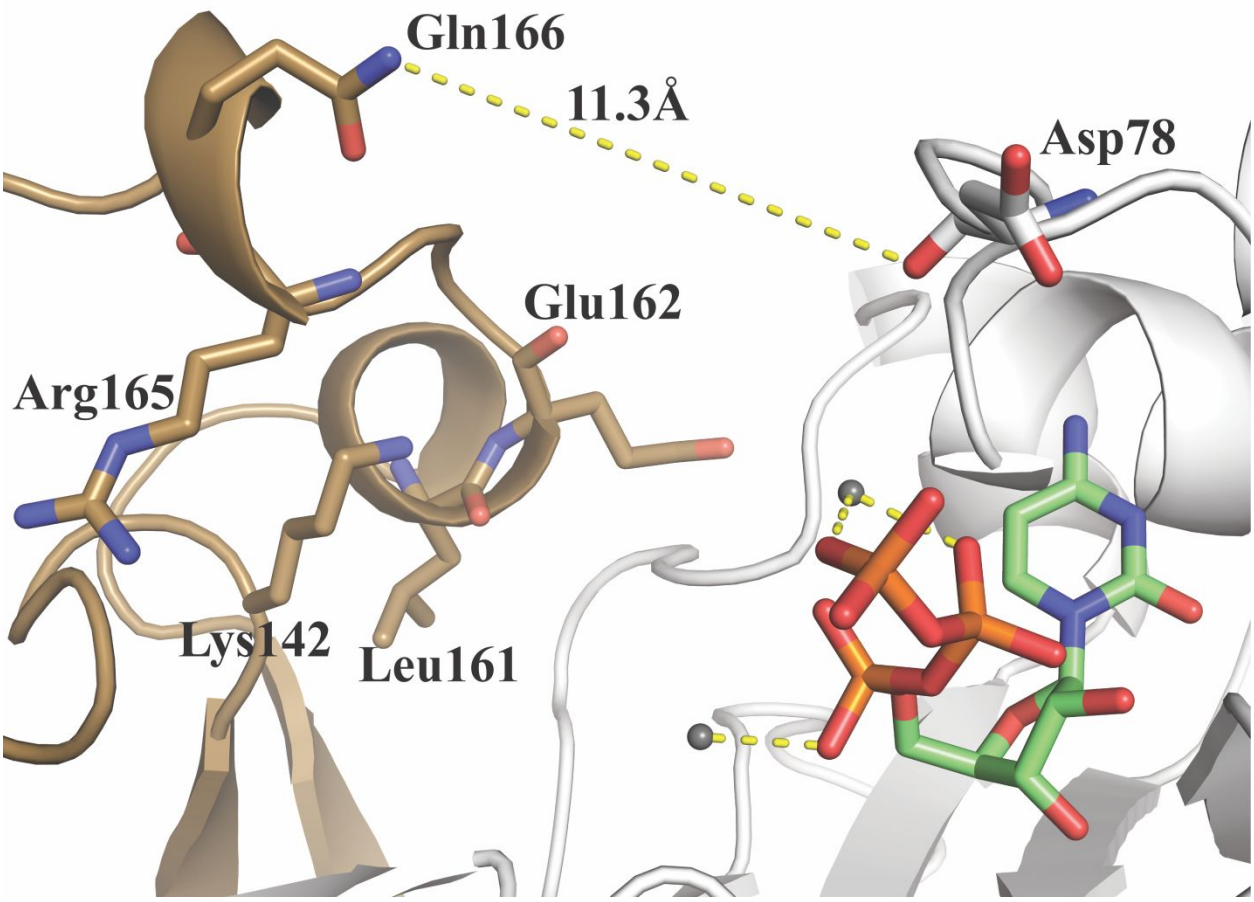

Figure3B

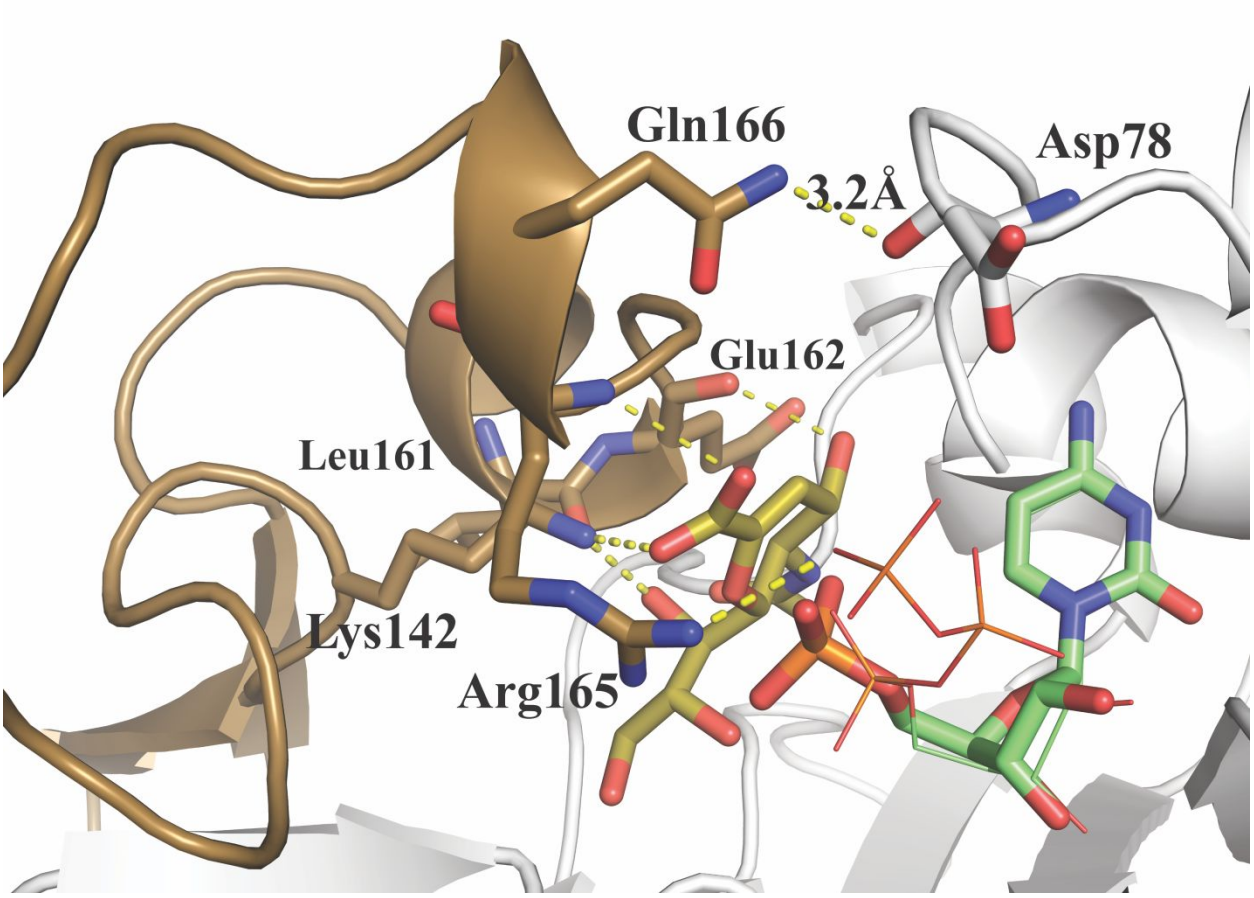

Figure 3C

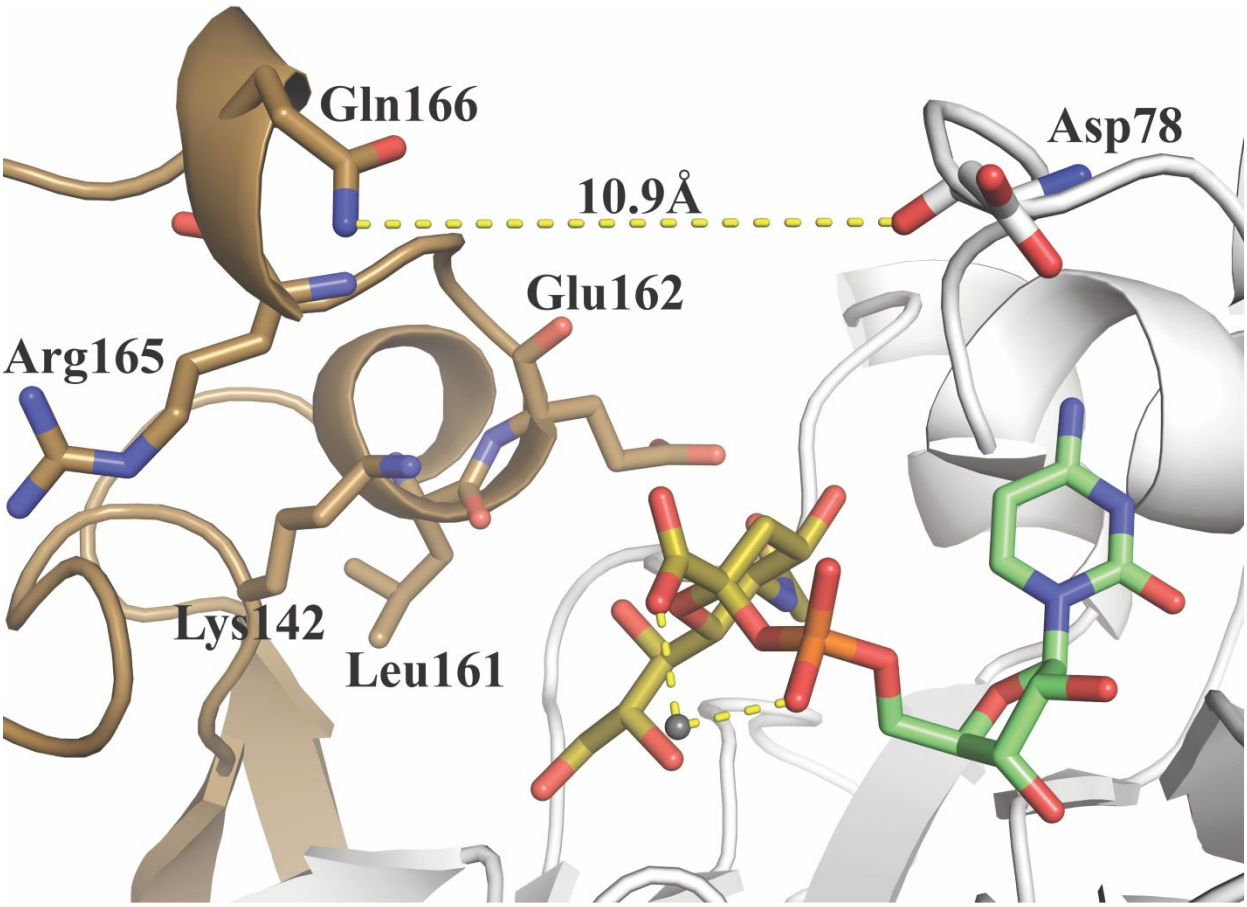

Figure 3D

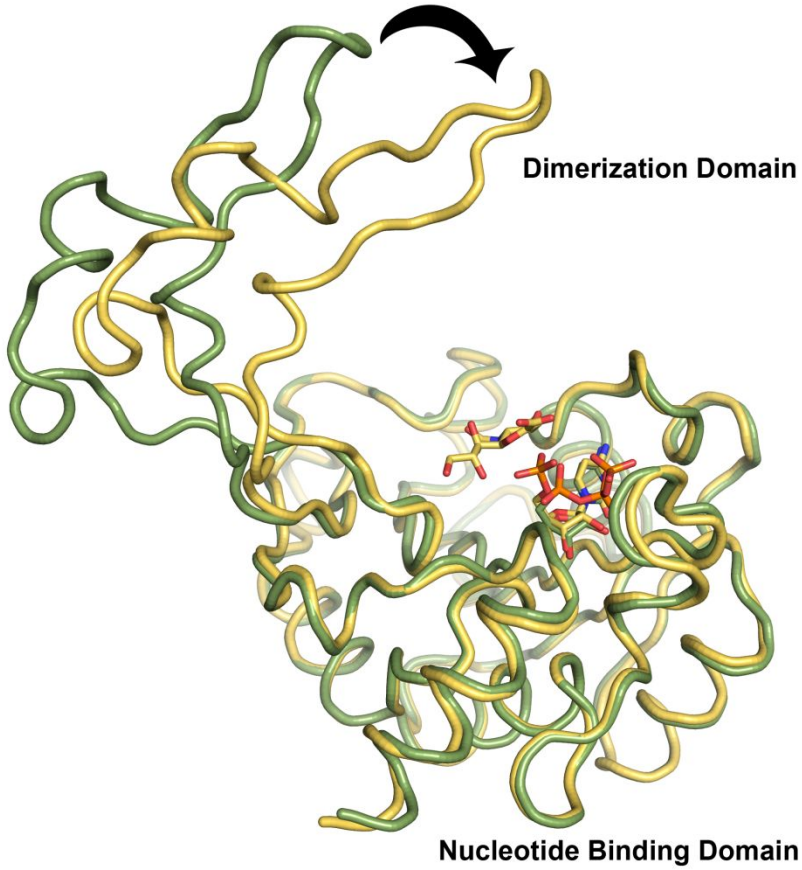


**Figure 3. Mechanism of active site closing.** (A)~~A~~, after CTP and $Ca^{2+}$ bind to monomer A, the enzyme maintains the open state until arrival of sialic acid. ~~B~~(B), as Neu5Ac2en binds to the nucleotide binding (NB) domain of monomer A (white), interactions involving 5 residues from the dimerization domain of monomer B (brown) and sialic acid (yellow sticks) cause the distance between dimerization and NB domain to decrease by up to 8 Å. ~~C~~(C), after formation of product, contacts between dimerization domain and sialic acid are broken, and the active site is re-opened. ~~D~~(D), superposition of nucleotide binding domains of the A monomers from CTP-bound structure (green) onto CMP- Neu5Ac2en structure (yellow). Relative orientation of the dimerization domain rotates closed upon binding Neu5Ac2en (highlighted by arrow).

Figure 4A

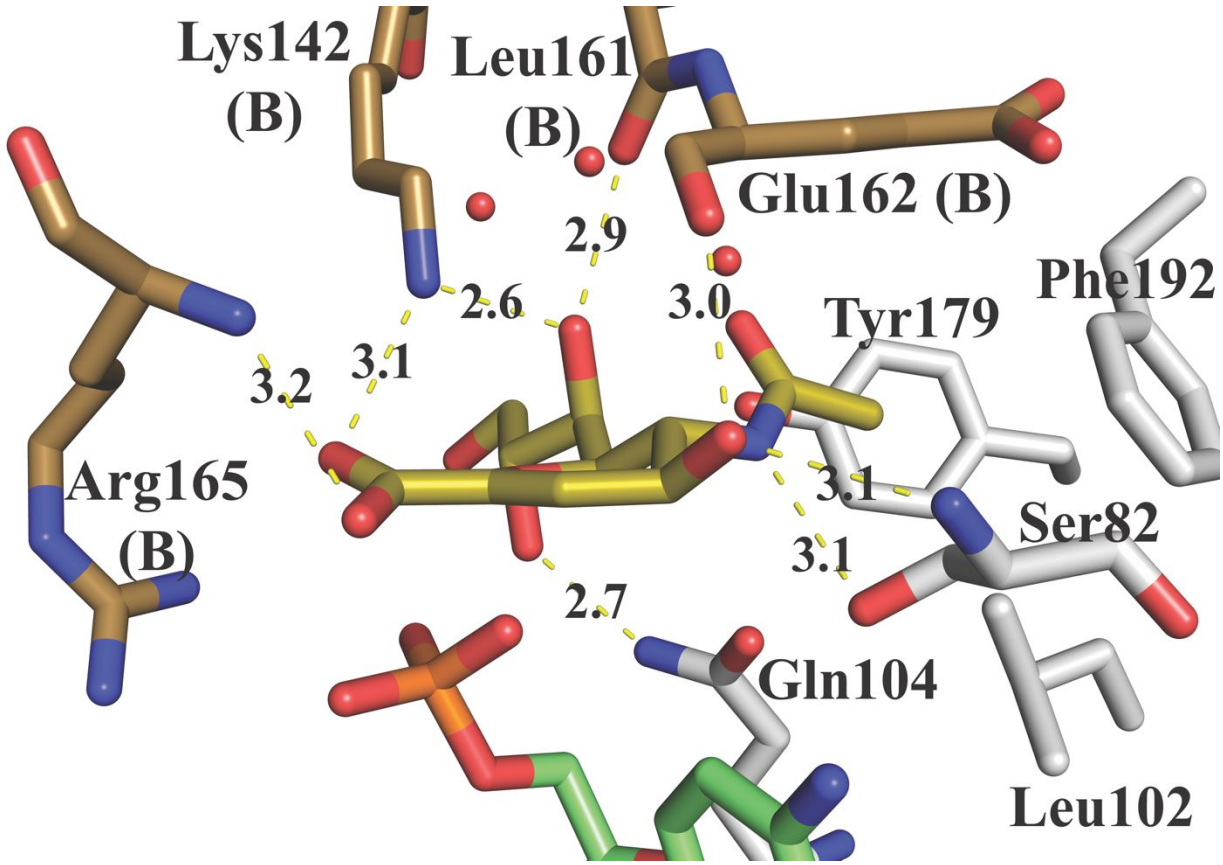
Lys142
(B)
Leu161
(B)
Glu162 (B)
2.9
2.6
3.0
Phe192
Tyr179
3.2
3.1
Arg165
(B)
3.1
Ser82
3.1
2.7
Gln104
Leu102

Figure 4B

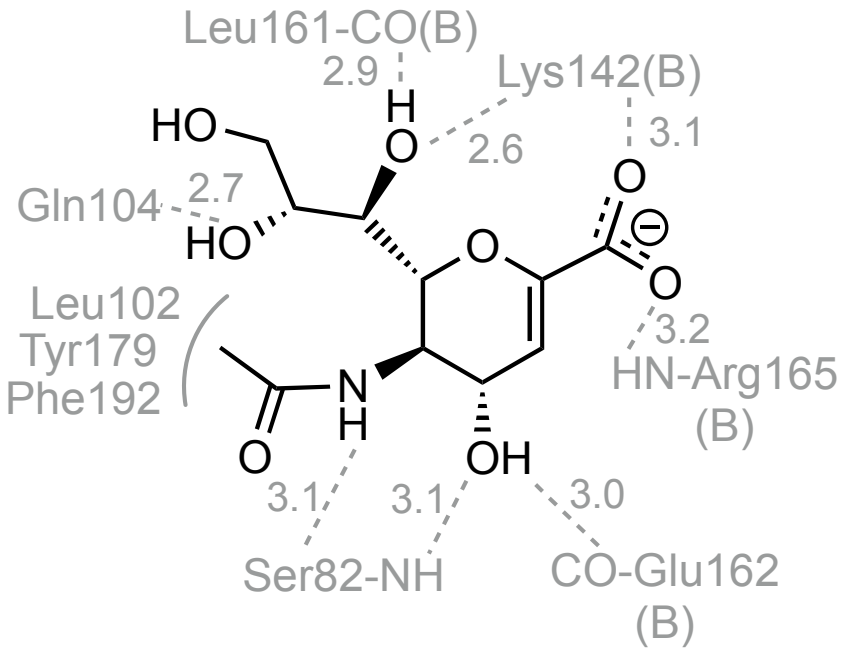


**Figure 4. Ligands involved in dimer closing.** ~~A~~(A), sialic acid analog (yellow) has numerous contacts with both the nucleotide-binding domain of monomer A (white sticks) and the dimerization domain of monomer B (brown sticks). Three ordered water molecules indicate a solvent pocket which may allow for substrate variation. ~~B~~(B), summary of contacts between NmCSS and Neu5Ac2en.

Figure 5

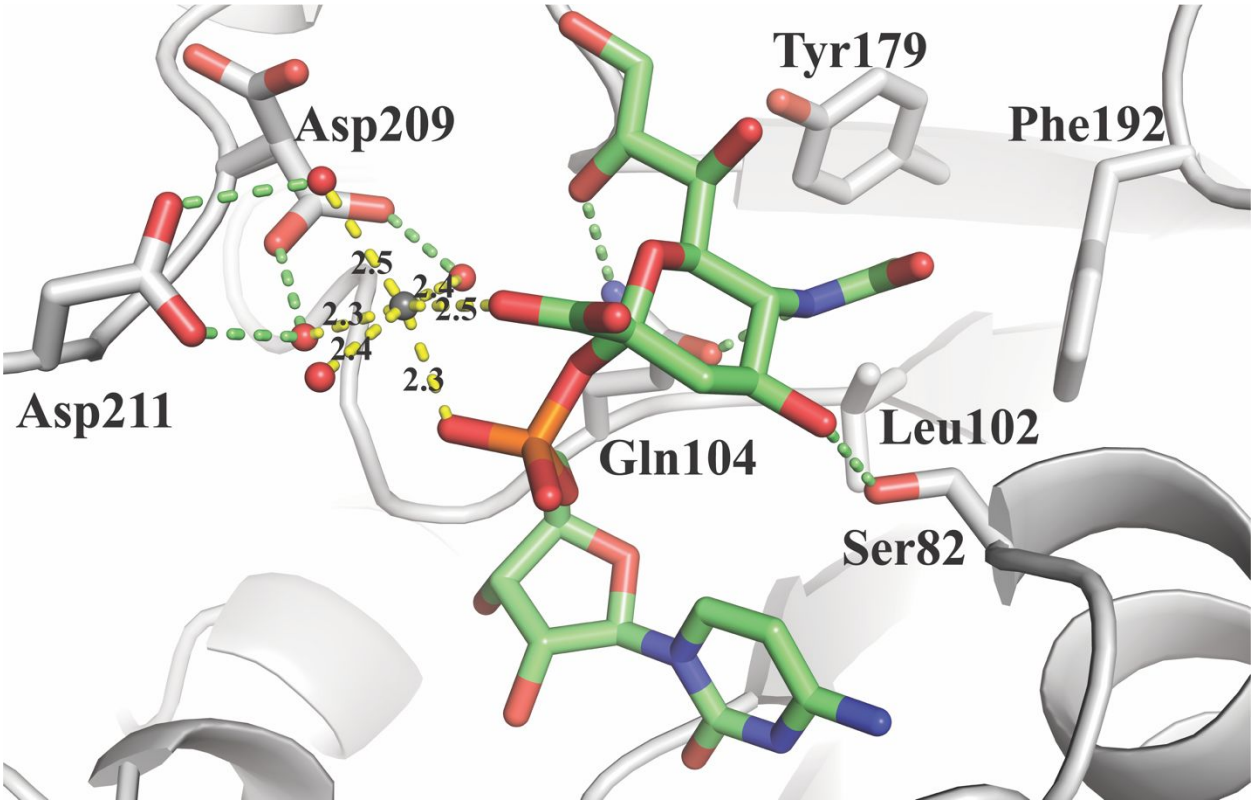


**Figure 5. Product-bound open state of NmCSS active site.** After CMP-Neu5Ac product formation (green-colored bonds), enzyme releases pyrophosphate and $Ca^{2+}$(B) and leaves behind $Ca^{2+}$–(A) and product. Interactions between sialic acid and the nucleotide binding domain are maintained, but those between sialic acid and the dimerization domain of the opposite monomer are broken.

Figure 6A

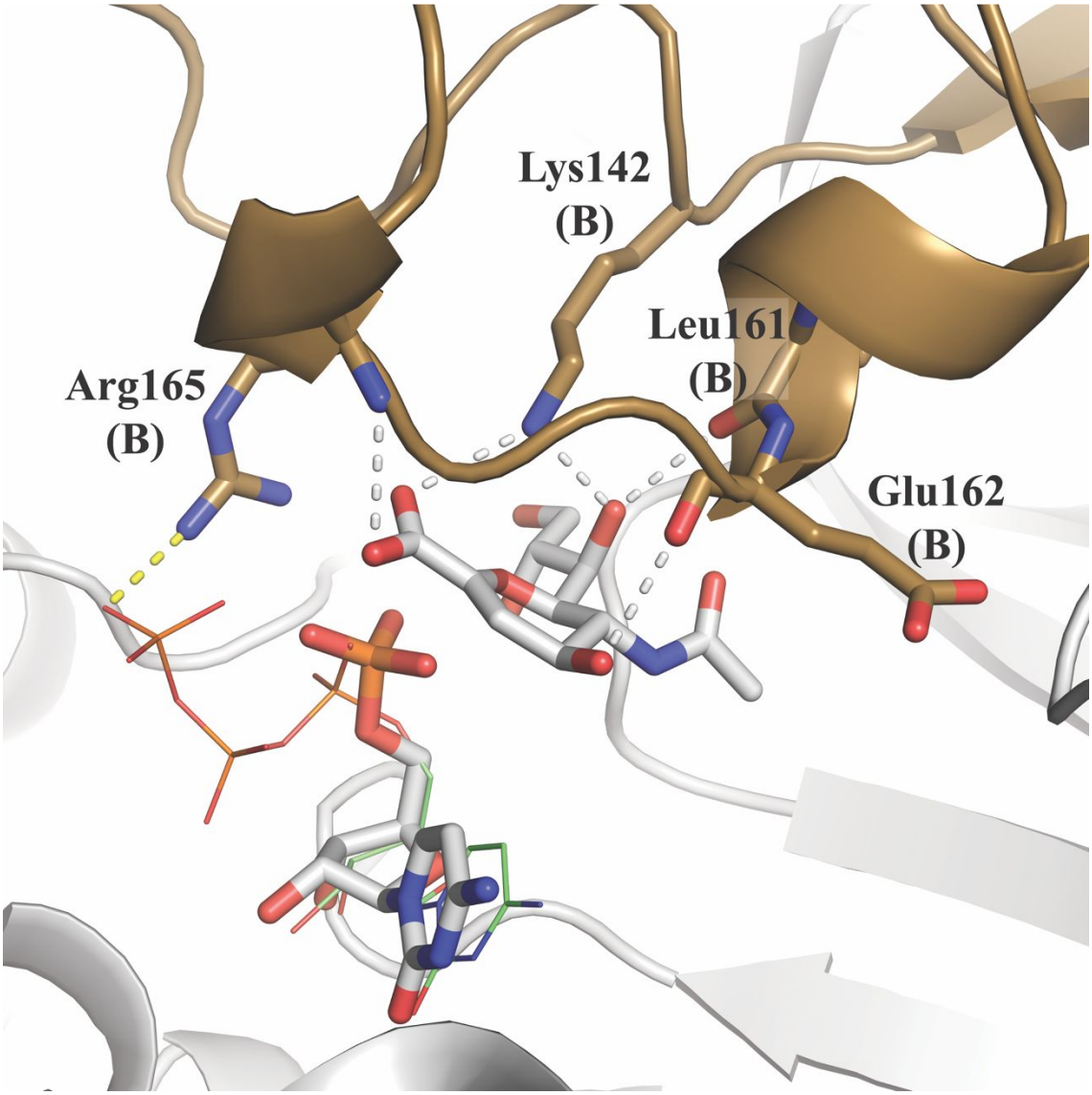

Figure 6B

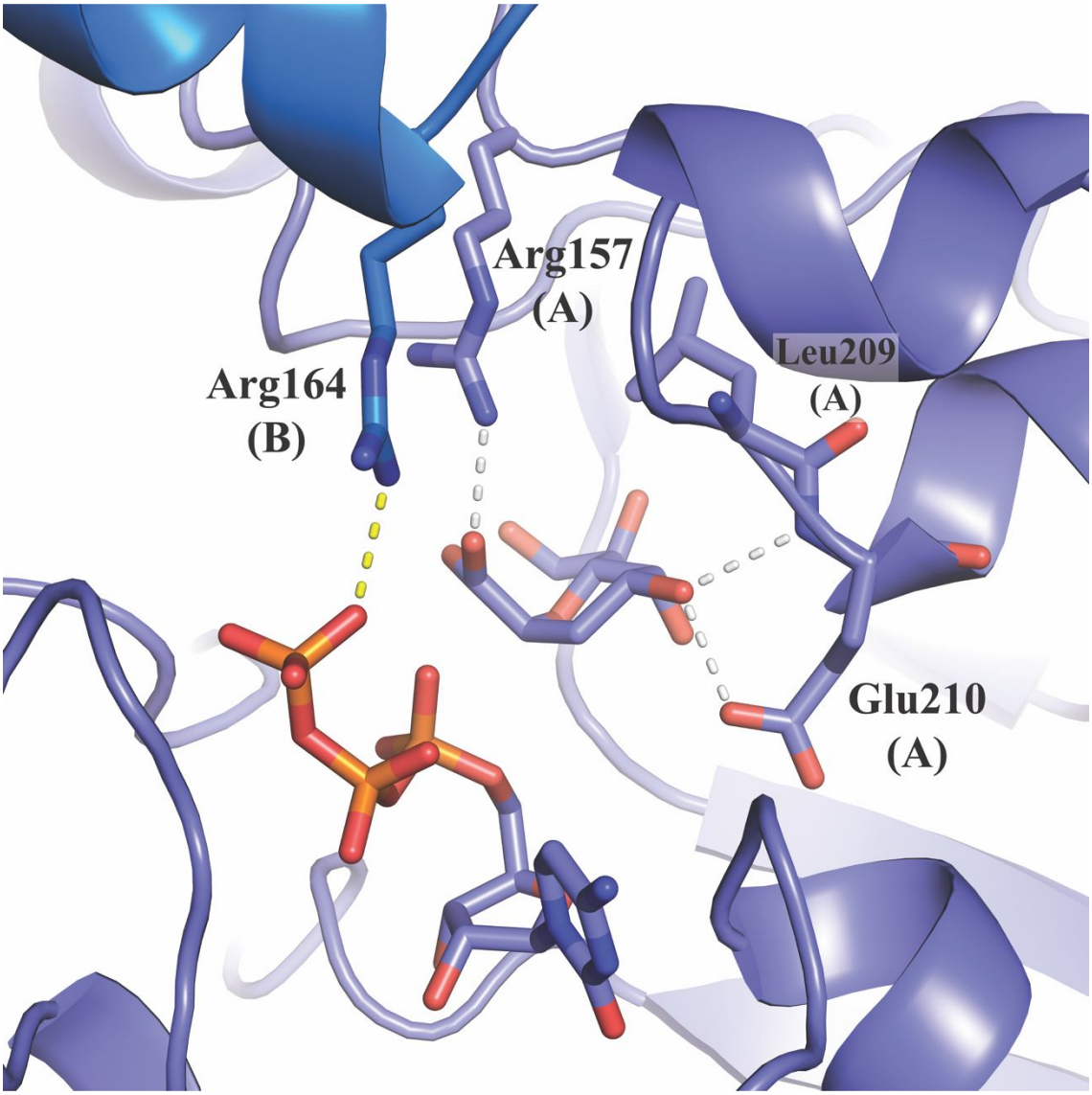

Figure 6C

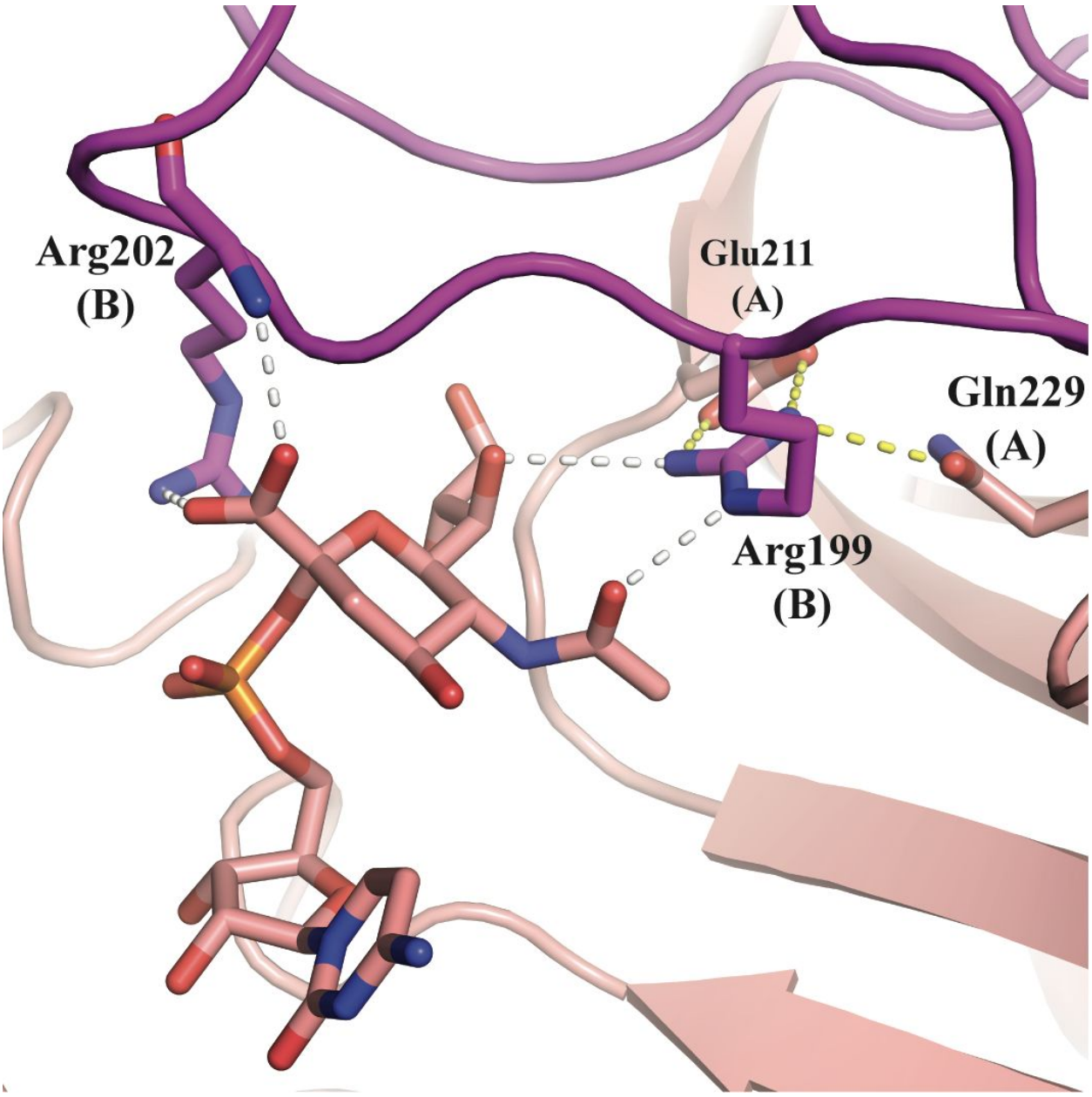


**Figure 6. Comparison of NmCSS to similar enzymes.** Interactions between protein and sugar are white dashes. Those between protein and nucleotide are yellow. ~~A~~(A), NmCSS:CMP:Neu5Ac2en with overlay of CTP (sticks) from NmCSS:CTP structure, highlighting residues from opposite monomer which interact with sialic acid and possibly with CTP. ~~B~~ (B) and ~~C~~ (C) focus on only a small selection of relevant protein-sugar interactions for comparison to

Lys142 and Arg165 of NmCSS. ~~B~~(B), EcKdsB:CTP:~~2-deoxy-~~Kdo2en (PDBID 3K8D). ~~2-deoxy-~~Kdo2en is a non-reacting analog of KdsB's natural substrate. ~~C~~(C), MmCSS:CMP-~~sialic acid~~Neu5Ac (PDBID 1QWJ). A bridging arginine between the dimerization domain and substrate of the opposite monomer is a common feature.

Figure 7A

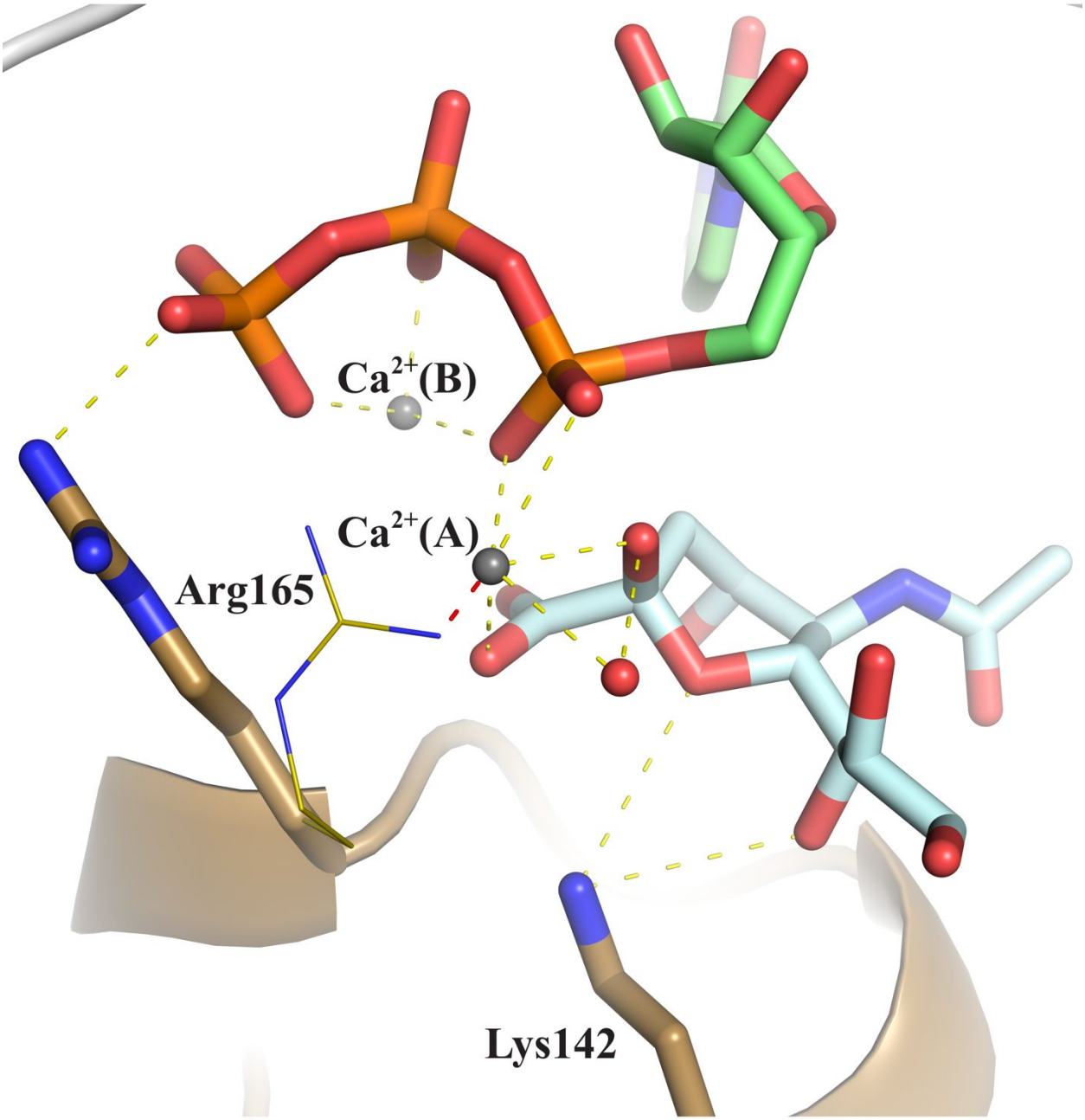

Figure 7B

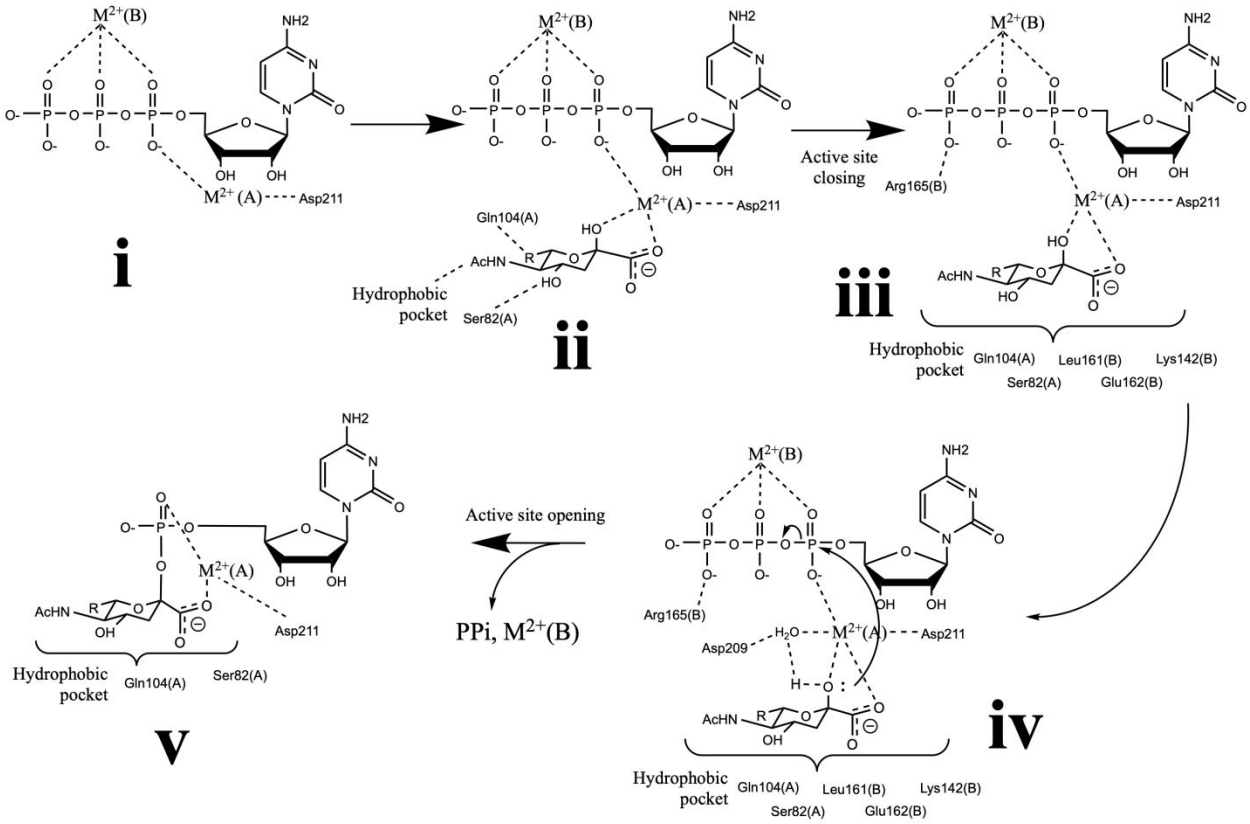


**Figure 7. Proposed mechanism of NmCSS.** ~~A~~(A), model of the NmCSS active site in the presence of both substrates. The conformation of CTP (green sticks) in the presence of $Ca^{2+}$(A) and $Ca^{2+}$(B) (gray spheres) superimposed into the NmCSS:CMP:Neu5Ac2en active site in which Neu5Ac2en has been replaced with Neu5Ac suggests a clash (red dashes) between $Ca^{2+}$(A) and Arg165 (thin brown sticks). However, a different rotamer of Arg165 (thick brown sticks) would allow for the observed $Ca^{2+}$(A) placement while preserving the negative-charge stabilization of CTP's γ-phosphate by the arginine guanidinium group. ~~B~~(B), **i**, CTP binds to the nucleotide binding (NB) domain first in addition to two divalent cations. **ii**, next, Neu5Ac enters the active site and associates initially with the NB domain but quickly (**iii**) draws together the NB and dimerization domains to form the closed state (all residues involved in Neu5Ac binding are

summarized below the structure for simplicity. **iv**, divalent cation $M^{2+}$ coordinates the C2-OH, allowing a water molecule to deprotonate C2-OH long enough for the hydroxyl O to attack the α-phosphate. **v**, after product formation, pyrophosphate ($PP_i$) and $M^{2+}$–(B) are released from the active site and the active site re-opens.

~~Supplemental~~ Figure S1

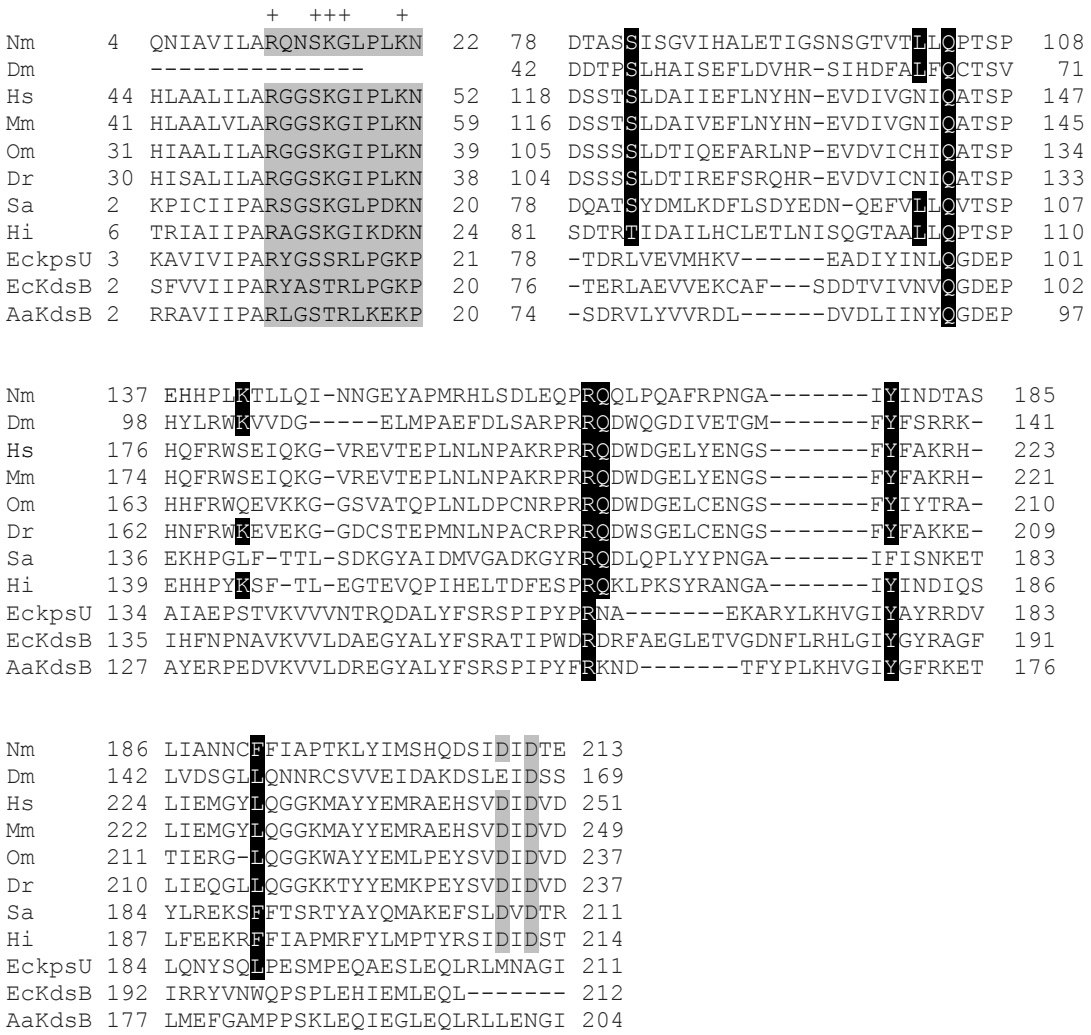


**~~Supplemental~~ Figure S1. Partial protein sequence ~~Alignment~~ alignment of CSS ~~senzymes~~.** *Neisseria meningitidis* (Nm), human (Hs), *Drosophila melanogaster* (Dm), mouse (Mm), rainbow trout (Om), zebra fish (Dr), *Streptococcus agalactiae* (Sa), *Haemophilus influenzae* (Hi), two *E. coli* CMP-Kdo synthetases (EckpsU and EcKdsB), and *Aquifex aeolicus* CMP-Kdo synthetase (AaKdsB). Conserved residues that interact with CTP in NmCSS are marked with a plus sign (+). Conserved residues involved in sialic binding in NmCSS are highlighted in black. P-loop residues are highlighted in dark gray. The conserved metal-binding motif DXD is highlighted in light gray.

~~Supplemental~~ Figure S2

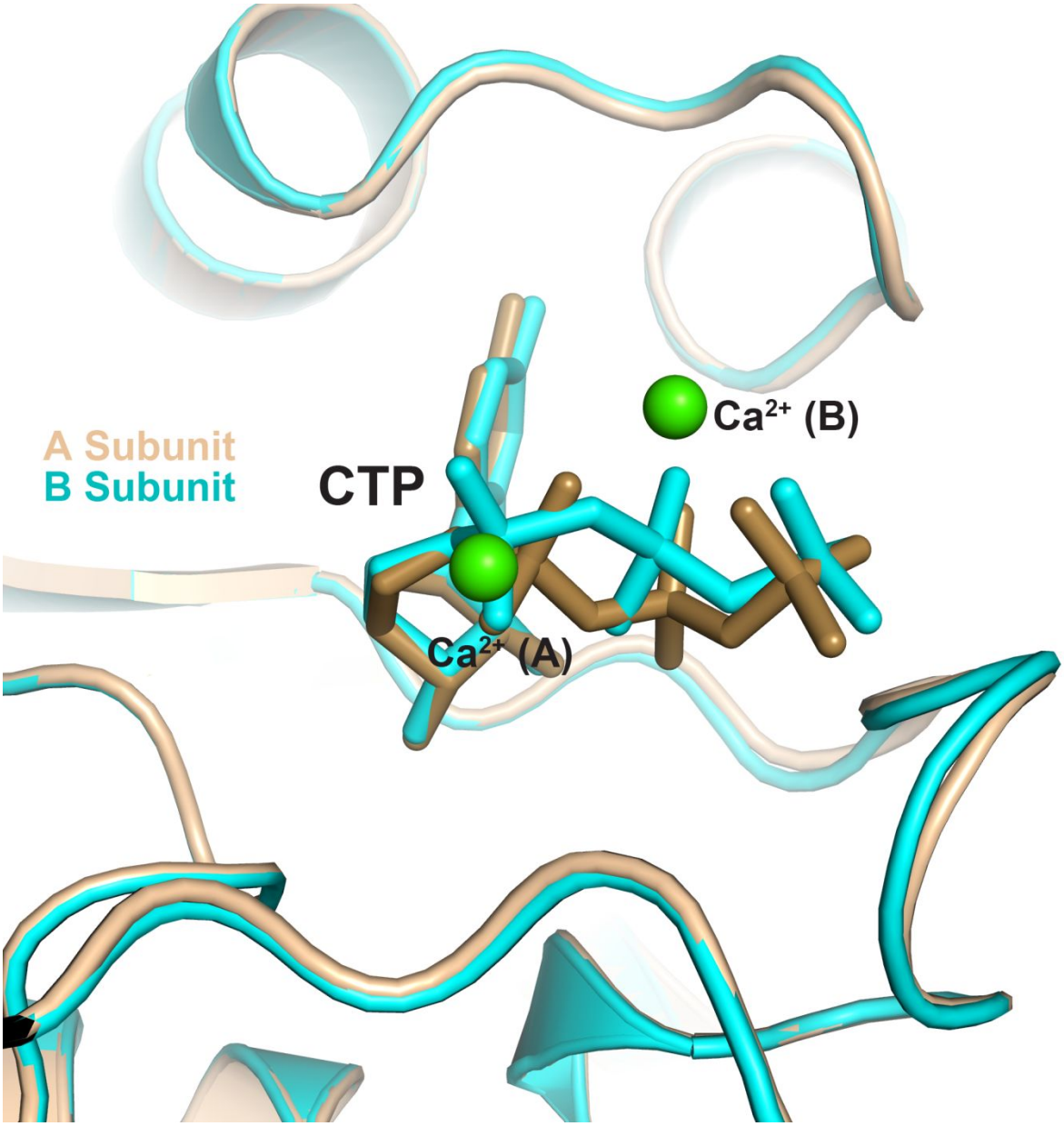


**~~Supplemental~~ Figure S2. Comparison of CTP binding between two monomers.** The two subunits in the asymmetric unit are superimposed highlighting the difference in the CTP triphosphate orientation. The A subunit CTP is shown in brown together with the two bound calcium ions, and the B subunit is shown in cyan, which binds CTP with no apparent calcium ligands. The electron density for the B subunit CTP β and γ phosphates is weaker than A subunit suggesting partial hydrolysis of CTP in the B subunit.

Figure S3

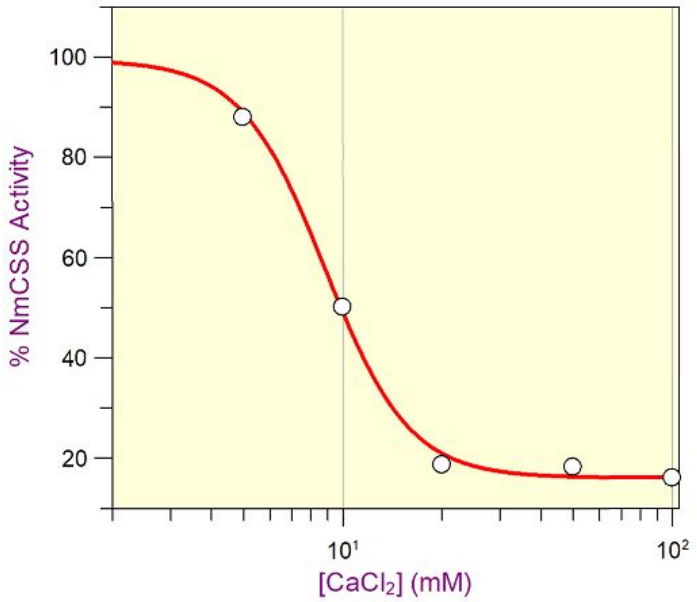


**Figure S3. Inhibition of NmCSS by $CaCl_2$.** Calculated $IC_{50}$ value is 8.8 ± 0.4 mM

Figure S4

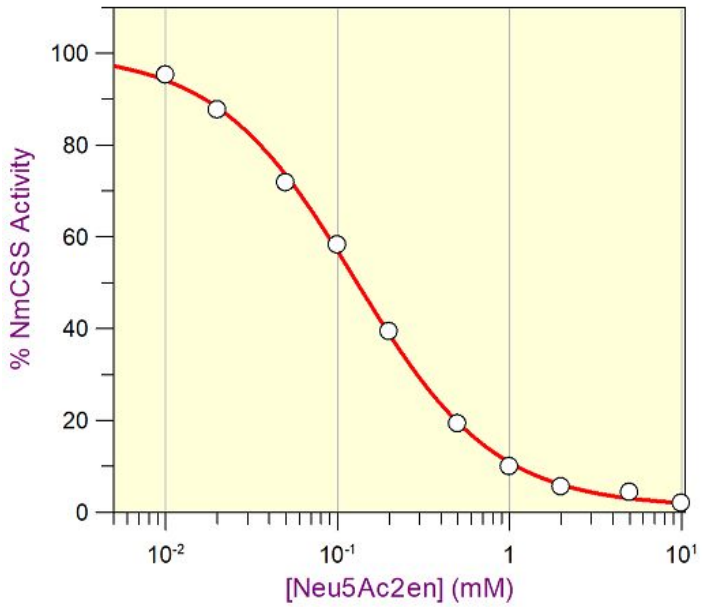


**Figure S4. Inhibition of NmCSS by Neu5Ac2en.** $IC_{50}$ value was calculated to be 0.13 ± 0.01 mM under the assay conditions.

~~Supplemental~~ Figure ~~3A~~S5A

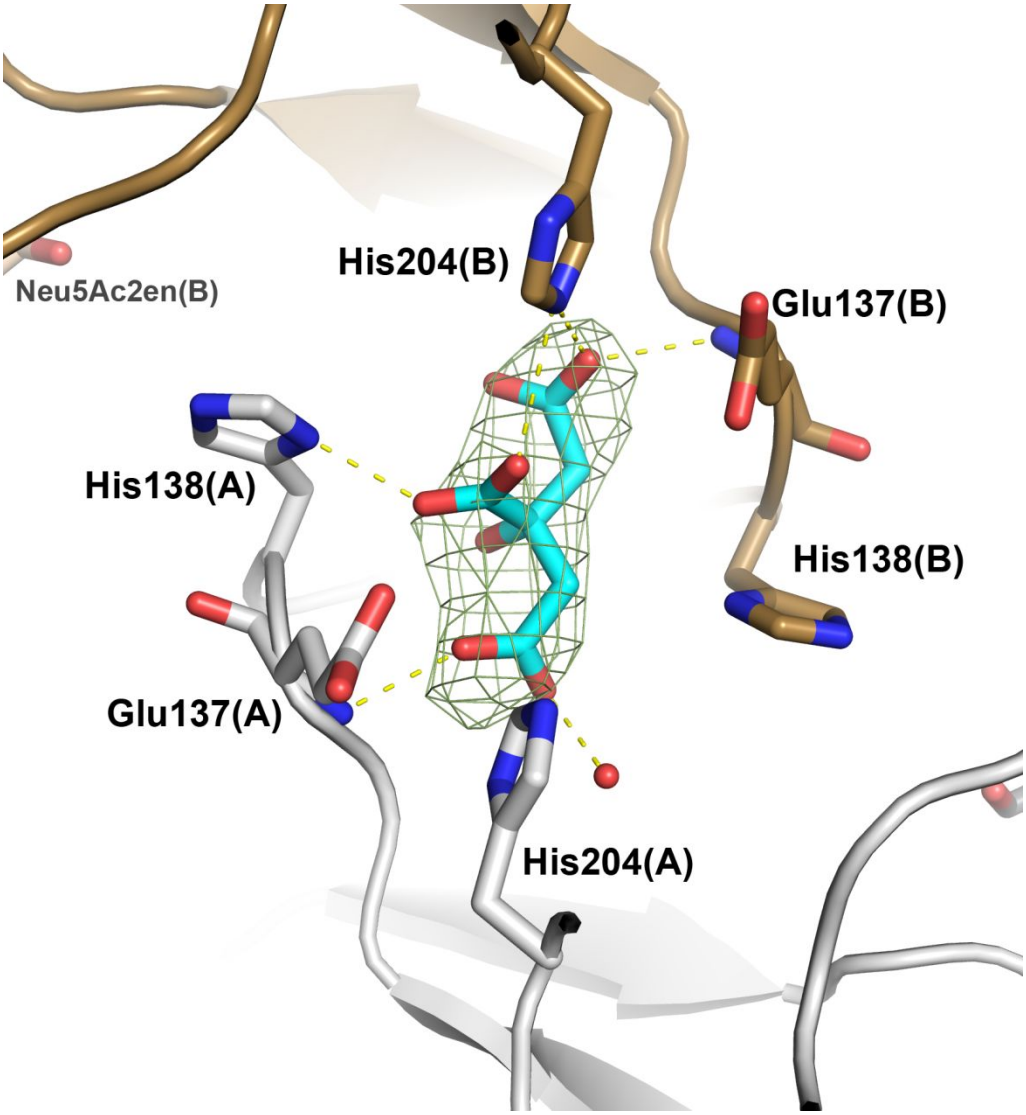

~~Supplemental~~ Figure ~~3B~~S5B

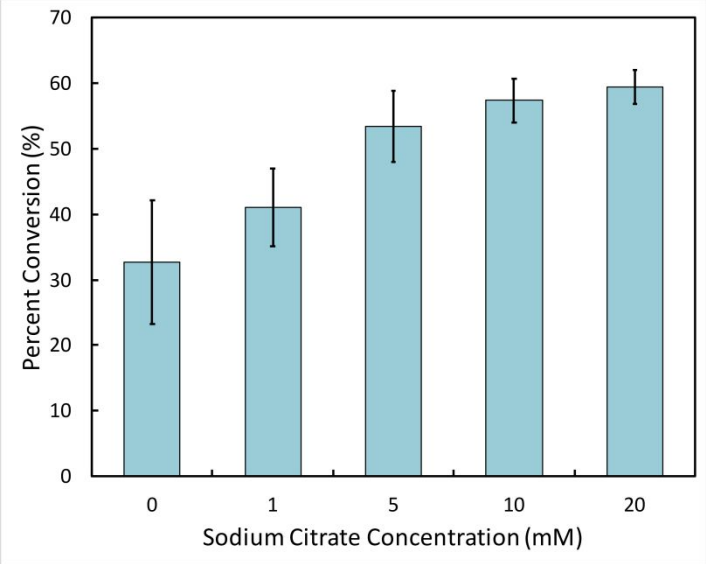


**~~Supplemental~~ Figure ~~3~~S5. Involvement of citrate in closed state stabilization.** ~~A~~(A), interactions between citrate (cyan) and enzyme are highlighted in yellow dashes. Fo-Fc difference electron density omit map is shown in green mesh contoured at 3.0σ. ~~B~~(B), activating effect of citrate on conversion of Neu5Ac to CMP-Neu5Ac by NmCSS.

**For Table of Contents Only**

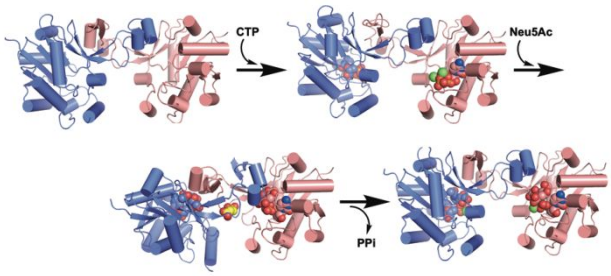

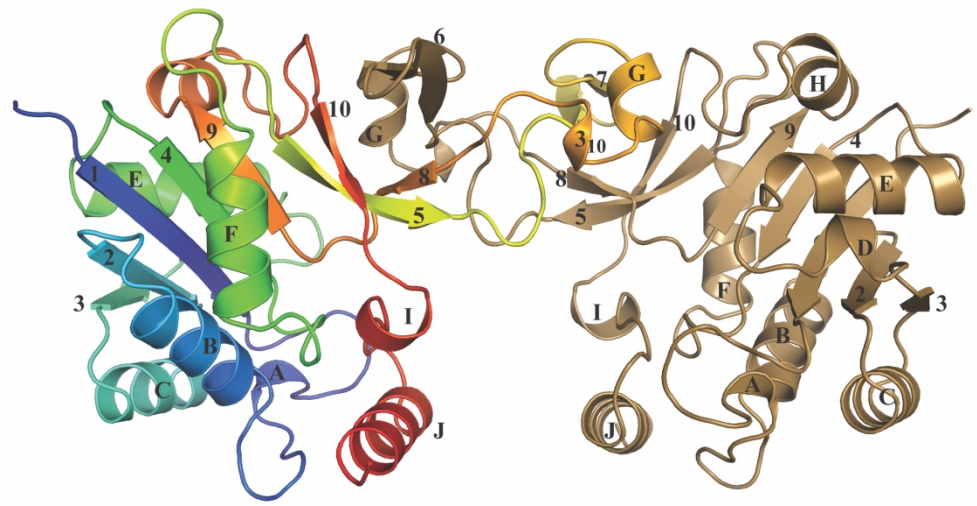


Figure 1. NmCSS homodimer structure. (A) Structure of ligand-free NmCSS homodimer. For contrast, one monomer is shown in bronze and the other in the rainbow spectrum starting with blue at the N-terminus and ending with red at the C-terminus. Each monomer consists of a globular nucleotide-binding domain and an extended dimerization domain where it interacts with its partner monomer. β-Sheets are labeled with numbers and α-helices with letters, with the exception of the $3_{10}$ helix located in the dimerization domain of each monomer. (B) Structure of NmCSS homodimer with ligands CMP and Neu5Ac2en bound in the active site, drawn as sticks with yellow- and green-colored carbon atoms respectively. Citrate binding at dimer interface is drawn in sticks with white-colored carbon atoms.

178x91mm (300 x 300 DPI)

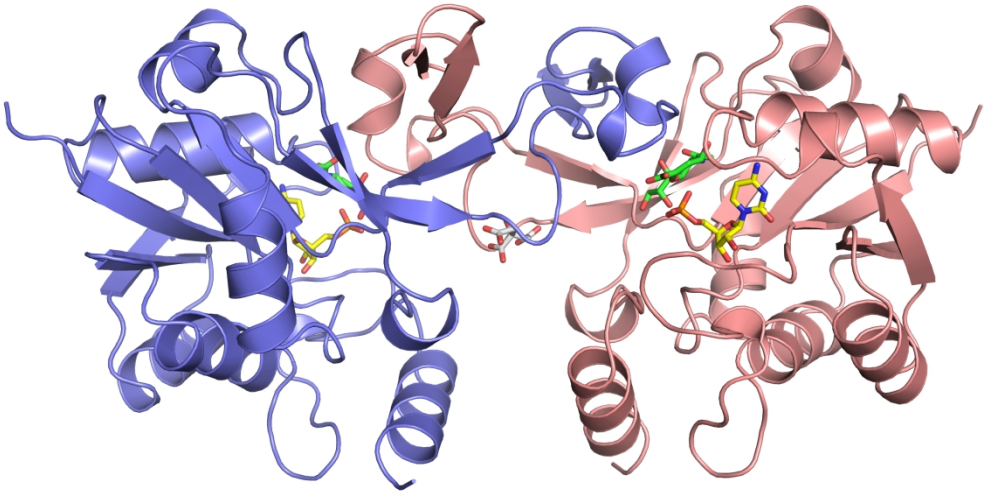

Figure 1. NmCSS homodimer structure. (A) Structure of ligand-free NmCSS homodimer. For contrast, one monomer is shown in bronze and the other in the rainbow spectrum starting with blue at the N-terminus and ending with red at the C-terminus. Each monomer consists of a globular nucleotide-binding domain and an extended dimerization domain where it interacts with its partner monomer. β-Sheets are labeled with numbers and α-helices with letters, with the exception of the $3_{10}$ helix located in the dimerization domain of each monomer. (B) Structure of NmCSS homodimer with ligands CMP and Neu5Ac2en bound in the active site, drawn as sticks with yellow- and green-colored carbon atoms respectively. Citrate binding at dimer interface is drawn in sticks with white-colored carbon atoms.

217x110mm (300 x 300 DPI)

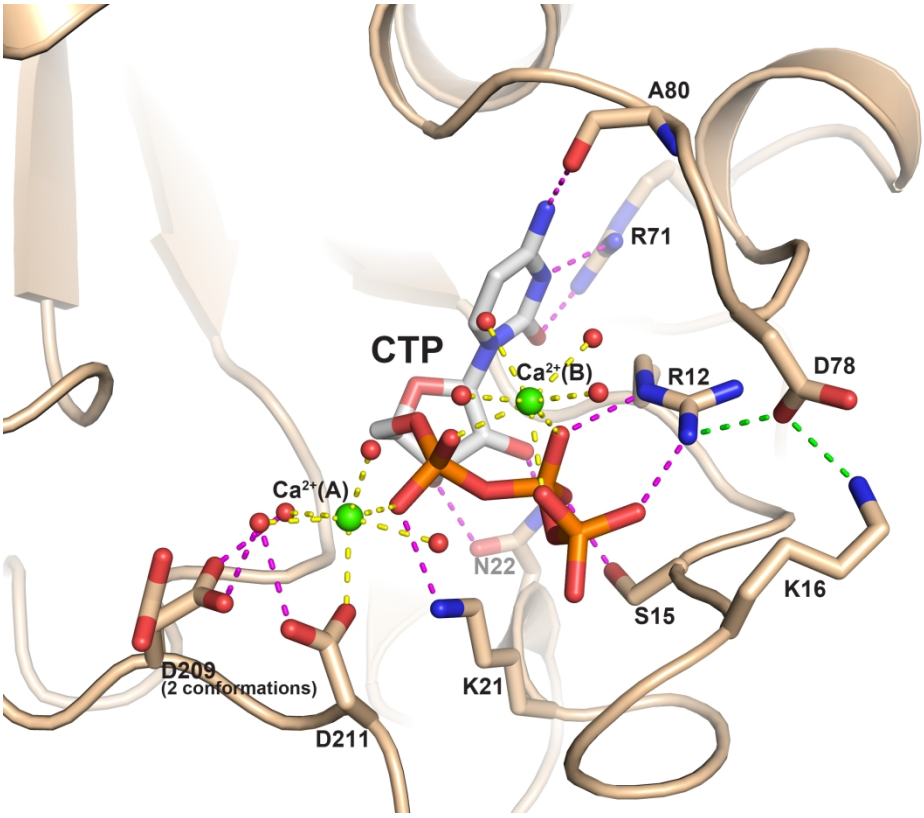


Figure 2. Binding orientation of CTP in the active site. CTP (white carbons) bound in the A subunit of the dimer with two calcium ions (green spheres) ligated to the phosphate moieties. Calcium ions (A) and (B) work together with the P-loop (residues 12-22) to properly position and stabilize the negative charge on the triphosphate group. Calcium ion A ligates to the α phosphate, Asp211, and four water molecules (red spheres). Asp209, which was observed to adopt two conformations with one binding to the $Ca^{2+}$(A) water ligands, together with Asp211 make up the conserved DXD motif. Calcium ion B ligates to all three phosphates of CTP together with four water molecules. Calcium ligations are highlighted with yellow dashed lines and hydrogen bonds between protein and Ca-CTP are magenta in color, while the P-loop stabilization interaction between Arg12-Asp78-Lys16 is drawn with green dashed lines.

460x371mm (149 x 149 DPI)

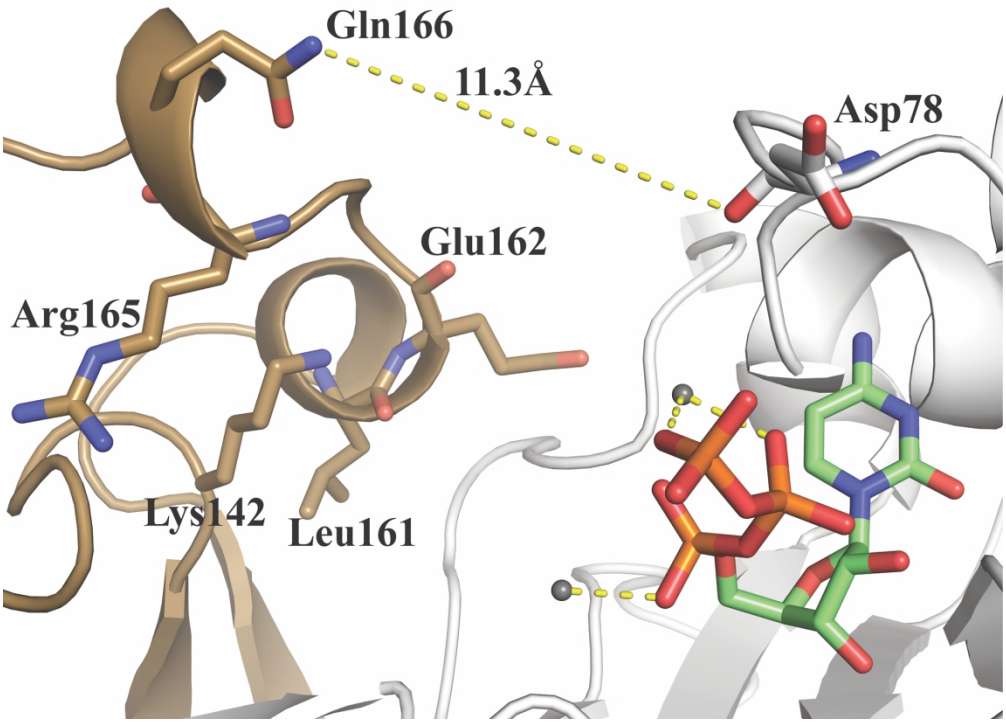


Figure 3. Mechanism of active site closing. (A), after CTP and $Ca^{2+}$ bind to monomer A, the enzyme maintains the open state until arrival of sialic acid. (B), as Neu5Ac2en binds to the nucleotide binding (NB) domain of monomer A (white), interactions involving 5 residues from the dimerization domain of monomer B (brown) and sialic acid (yellow sticks) cause the distance between dimerization and NB domain to decrease by up to 8 Å. (C), after formation of product, contacts between dimerization domain and sialic acid are broken, and the active site is re-opened. (D), superposition of nucleotide binding domains of the A monomers from CTP-bound structure (green) onto CMP- Neu5Ac2en structure (yellow). Relative orientation of the dimerization domain rotates closed upon binding Neu5Ac2en (highlighted by arrow).

179x129mm (300 x 300 DPI)

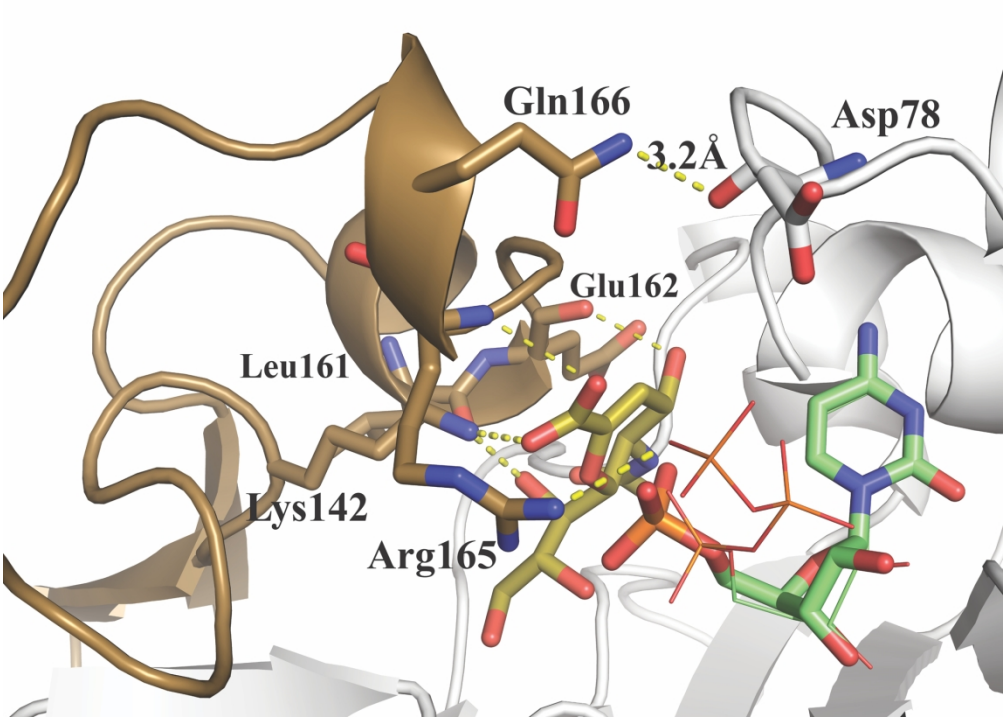


Figure 3. Mechanism of active site closing. (A), after CTP and $Ca^{2+}$ bind to monomer A, the enzyme maintains the open state until arrival of sialic acid. (B), as Neu5Ac2en binds to the nucleotide binding (NB) domain of monomer A (white), interactions involving 5 residues from the dimerization domain of monomer B (brown) and sialic acid (yellow sticks) cause the distance between dimerization and NB domain to decrease by up to 8 Å. (C), after formation of product, contacts between dimerization domain and sialic acid are broken, and the active site is re-opened. (D), superposition of nucleotide binding domains of the A monomers from CTP-bound structure (green) onto CMP- Neu5Ac2en structure (yellow). Relative orientation of the dimerization domain rotates closed upon binding Neu5Ac2en (highlighted by arrow).

179x129mm (300 x 300 DPI)

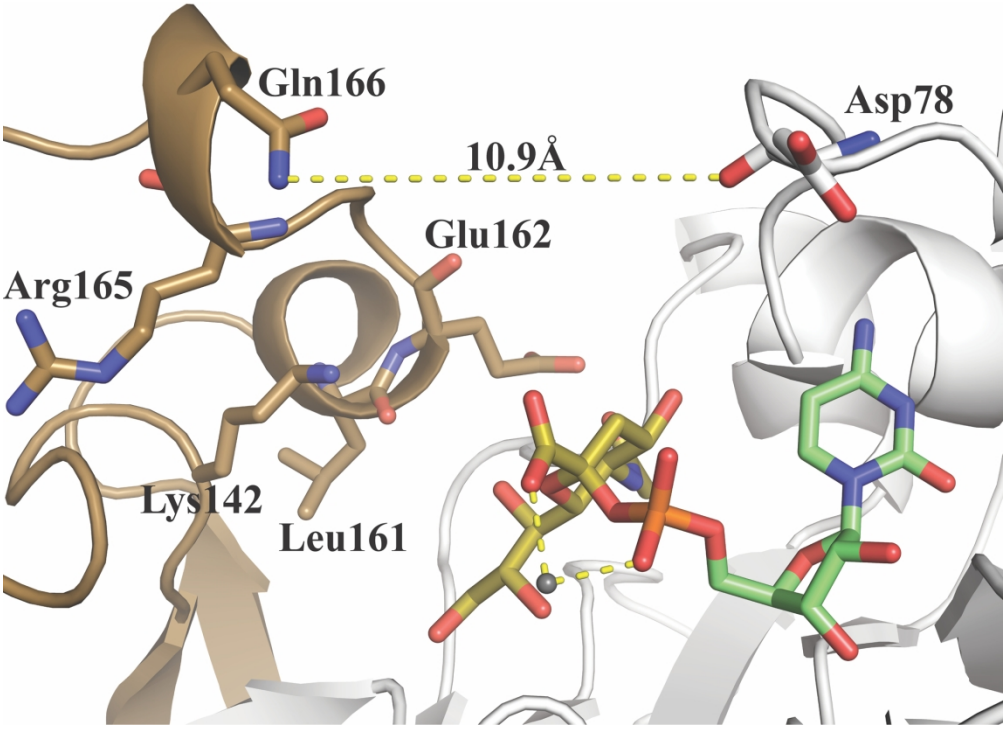


Figure 3. Mechanism of active site closing. (A), after CTP and $Ca^{2+}$ bind to monomer A, the enzyme maintains the open state until arrival of sialic acid. (B), as Neu5Ac2en binds to the nucleotide binding (NB) domain of monomer A (white), interactions involving 5 residues from the dimerization domain of monomer B (brown) and sialic acid (yellow sticks) cause the distance between dimerization and NB domain to decrease by up to 8 Å. (C), after formation of product, contacts between dimerization domain and sialic acid are broken, and the active site is re-opened. (D), superposition of nucleotide binding domains of the A monomers from CTP-bound structure (green) onto CMP- Neu5Ac2en structure (yellow). Relative orientation of the dimerization domain rotates closed upon binding Neu5Ac2en (highlighted by arrow).

179x129mm (300 x 300 DPI)

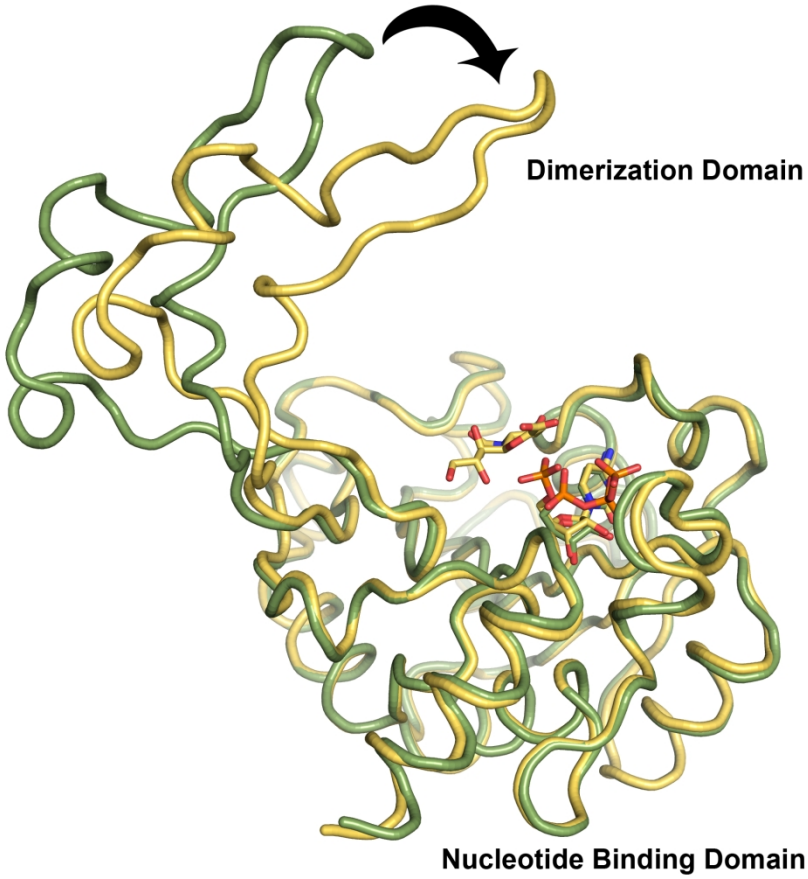


Figure 3. Mechanism of active site closing. (A), after CTP and $Ca^{2+}$ bind to monomer A, the enzyme maintains the open state until arrival of sialic acid. (B), as Neu5Ac2en binds to the nucleotide binding (NB) domain of monomer A (white), interactions involving 5 residues from the dimerization domain of monomer B (brown) and sialic acid (yellow sticks) cause the distance between dimerization and NB domain to decrease by up to 8 Å. (C), after formation of product, contacts between dimerization domain and sialic acid are broken, and the active site is re-opened. (D), superposition of nucleotide binding domains of the A monomers from CTP-bound structure (green) onto CMP- Neu5Ac2en structure (yellow). Relative orientation of the dimerization domain rotates closed upon binding Neu5Ac2en (highlighted by arrow).

381x350mm (149 x 149 DPI)

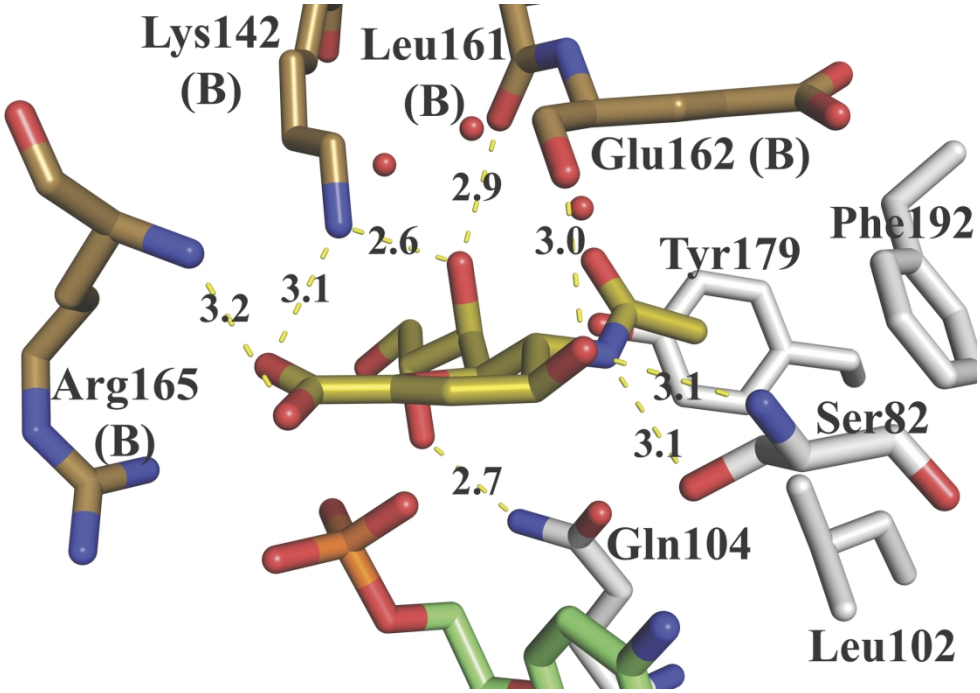


Figure 4. Ligands involved in dimer closing. (A), sialic acid analog (yellow) has numerous contacts with both the nucleotide-binding domain of monomer A (white sticks) and the dimerization domain of monomer B (brown sticks). Three ordered water molecules indicate a solvent pocket which may allow for substrate variation. (B), summary of contacts between NmCSS and Neu5Ac2en.

179x123mm (300 x 300 DPI)

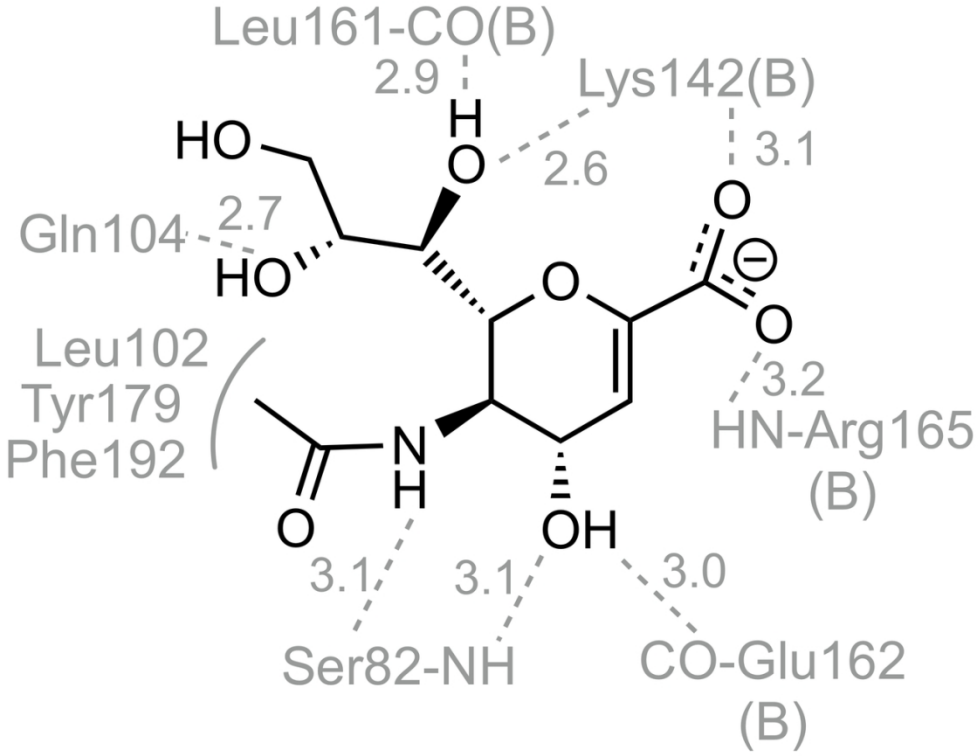


Figure 4. Ligands involved in dimer closing. (A), sialic acid analog (yellow) has numerous contacts with both the nucleotide-binding domain of monomer A (white sticks) and the dimerization domain of monomer B (brown sticks). Three ordered water molecules indicate a solvent pocket which may allow for substrate variation. (B), summary of contacts between NmCSS and Neu5Ac2en.

113x88mm (300 x 300 DPI)

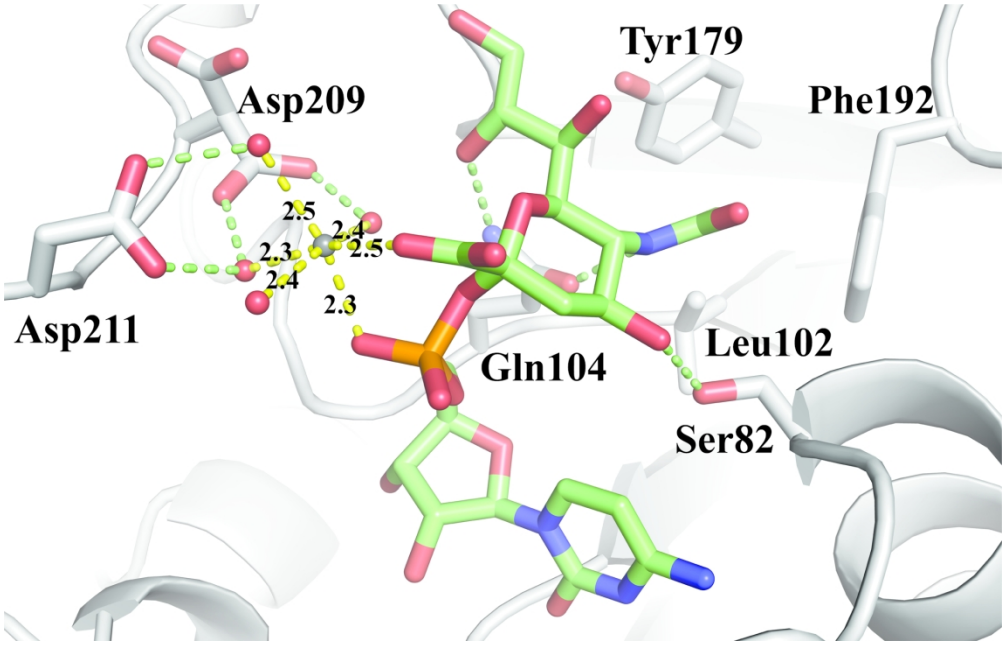


Figure 5. Product-bound open state of NmCSS active site. After CMP-Neu5Ac product formation (green-colored bonds), enzyme releases pyrophosphate and $Ca^{2+}$(B) and leaves behind $Ca^{2+}$(A) and product. Interactions between sialic acid and the nucleotide binding domain are maintained, but those between sialic acid and the dimerization domain of the opposite monomer are broken.

180x114mm (300 x 300 DPI)

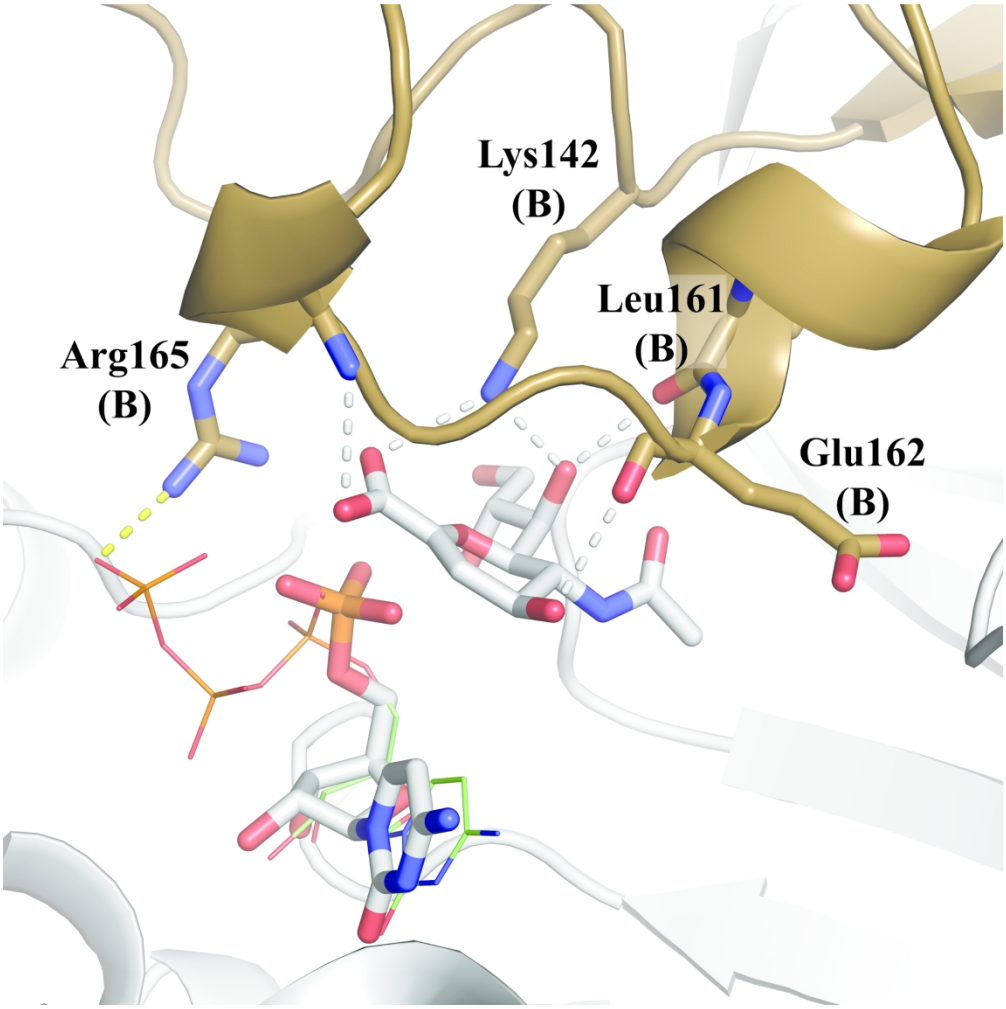


Figure 6. Comparison of NmCSS to similar enzymes. Interactions between protein and sugar are white dashes. Those between protein and nucleotide are yellow. (A), NmCSS:CMP:Neu5Ac2en with overlay of CTP (sticks) from NmCSS:CTP structure, highlighting residues from opposite monomer which interact with sialic acid and possibly with CTP. (B) and (C) focus on only a small selection of relevant protein-sugar interactions for comparison to Lys142 and Arg165 of NmCSS. (B), EcKdsB:CTP:Kdo2en (PDBID 3K8D). Kdo2en is a non-reacting analog of KdsB's natural substrate. (C), MmCSS:CMP-Neu5Ac (PDBID 1QWJ). A bridging arginine between the dimerization domain and substrate of the opposite monomer is a common feature.

180x180mm (300 x 300 DPI)

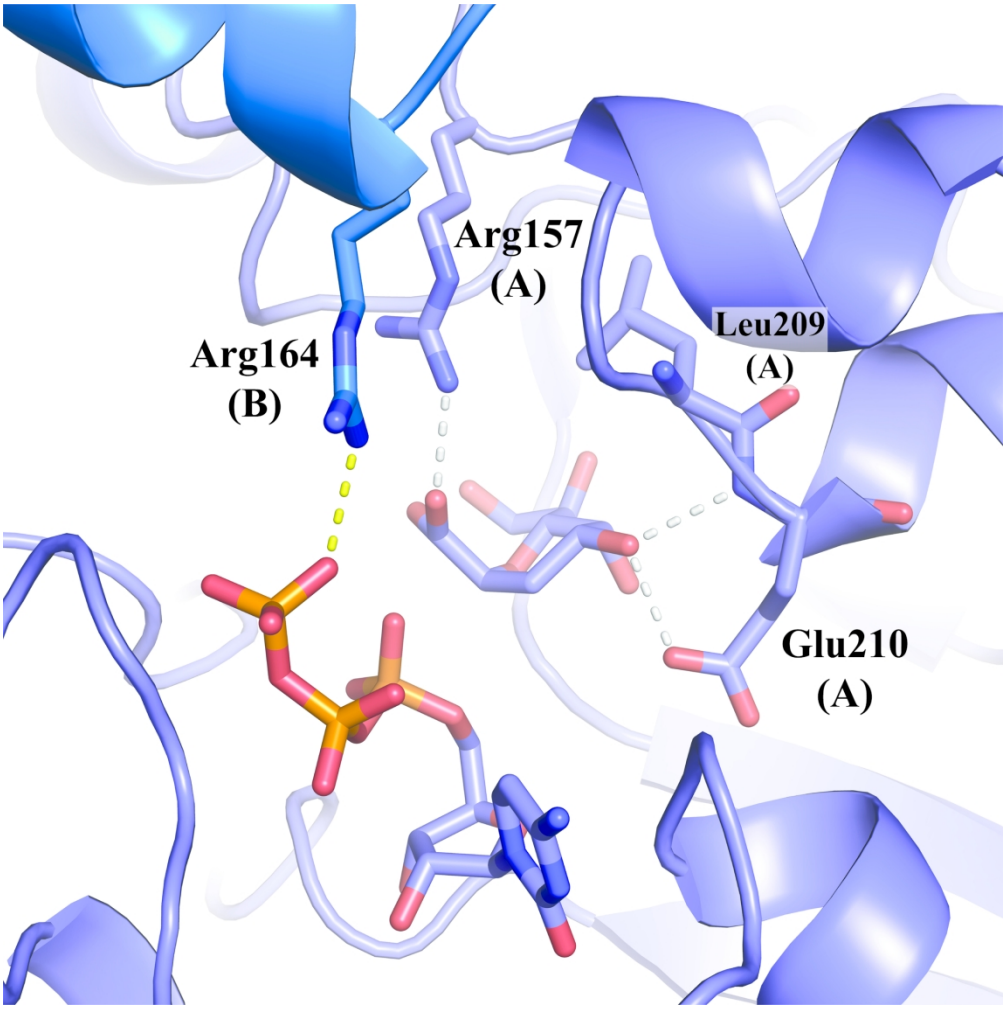


Figure 6. Comparison of NmCSS to similar enzymes. Interactions between protein and sugar are white dashes. Those between protein and nucleotide are yellow. (A), NmCSS:CMP:Neu5Ac2en with overlay of CTP (sticks) from NmCSS:CTP structure, highlighting residues from opposite monomer which interact with sialic acid and possibly with CTP. (B) and (C) focus on only a small selection of relevant protein-sugar interactions for comparison to Lys142 and Arg165 of NmCSS. (B), EcKdsB:CTP:Kdo2en (PDBID 3K8D). Kdo2en is a non-reacting analog of KdsB's natural substrate. (C), MmCSS:CMP-Neu5Ac (PDBID 1QWJ). A bridging arginine between the dimerization domain and substrate of the opposite monomer is a common feature.

180x180mm (300 x 300 DPI)

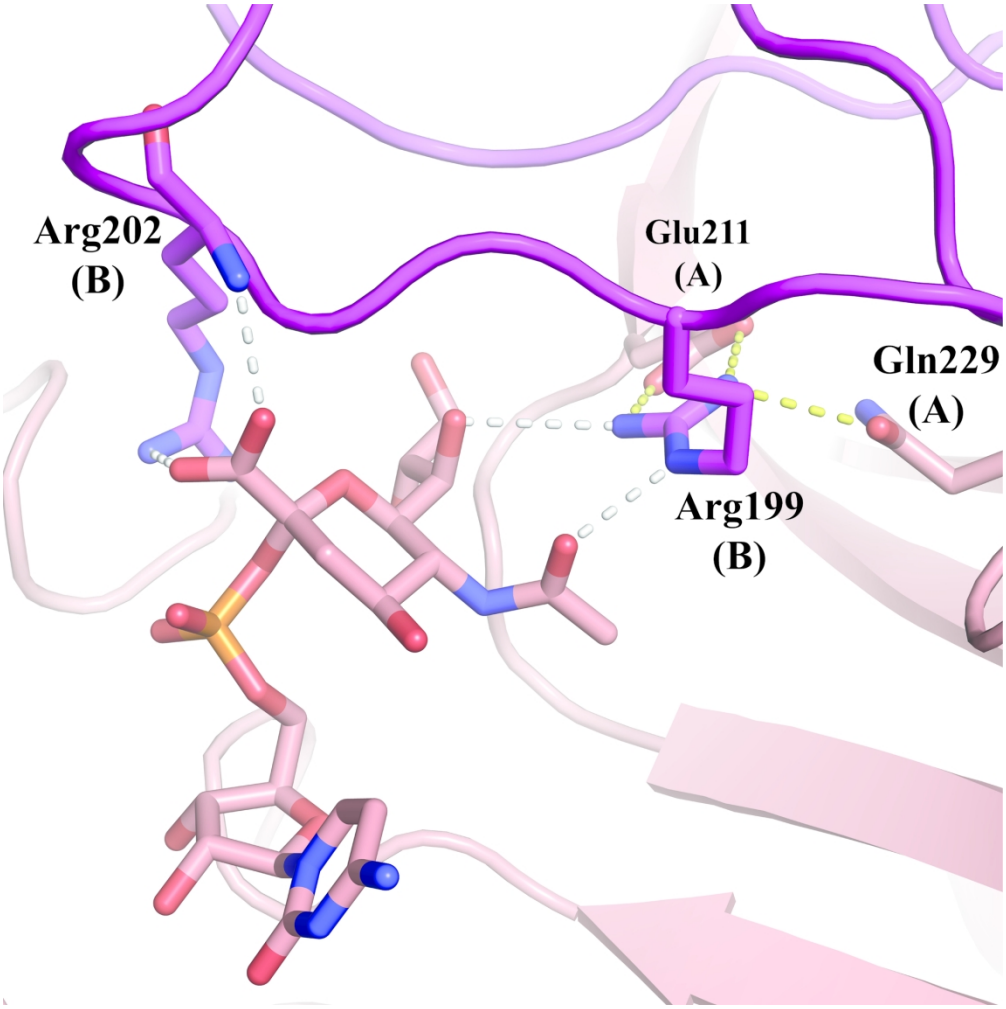


Figure 6. Comparison of NmCSS to similar enzymes. Interactions between protein and sugar are white dashes. Those between protein and nucleotide are yellow. (A), NmCSS:CMP:Neu5Ac2en with overlay of CTP (sticks) from NmCSS:CTP structure, highlighting residues from opposite monomer which interact with sialic acid and possibly with CTP. (B) and (C) focus on only a small selection of relevant protein-sugar interactions for comparison to Lys142 and Arg165 of NmCSS. (B), EcKdsB:CTP:Kdo2en (PDBID 3K8D). Kdo2en is a non-reacting analog of KdsB's natural substrate. (C), MmCSS:CMP-Neu5Ac (PDBID 1QWJ). A bridging arginine between the dimerization domain and substrate of the opposite monomer is a common feature.

180x180mm (300 x 300 DPI)

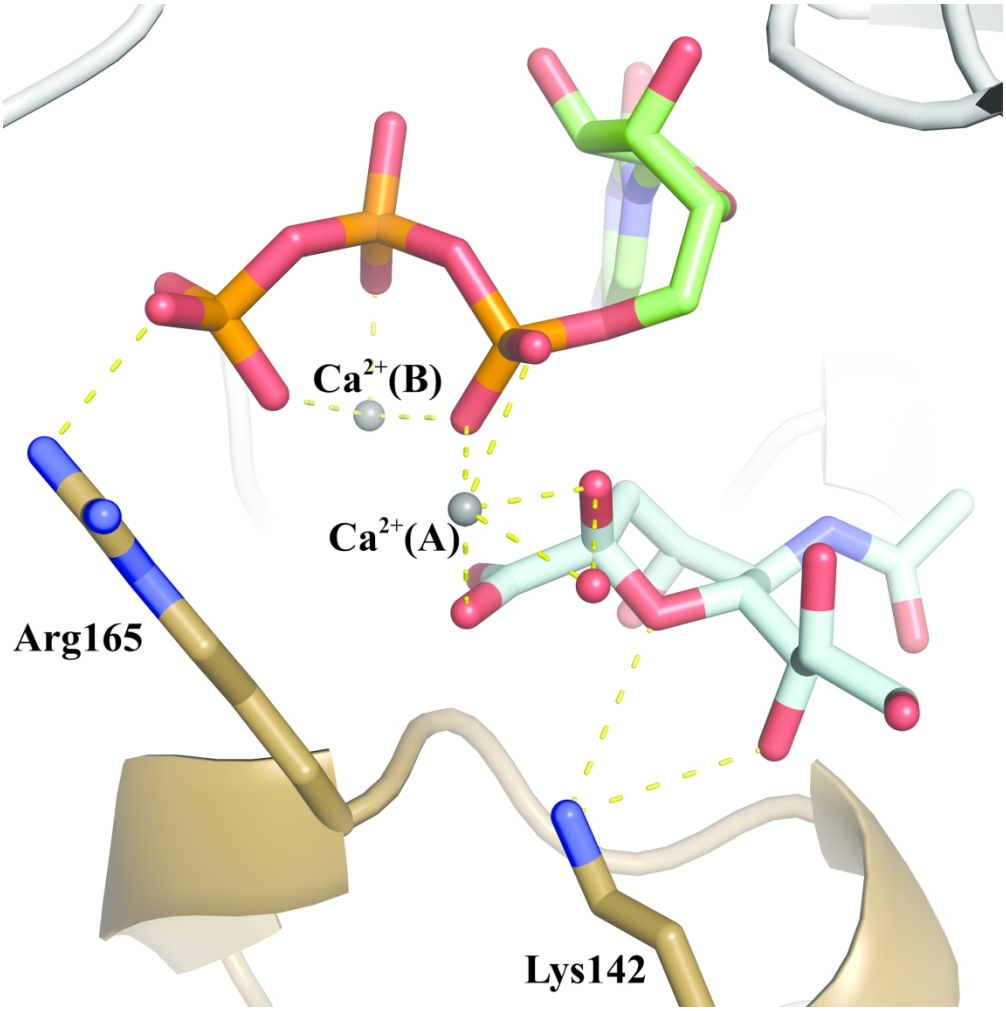


Figure 7. Proposed mechanism of NmCSS. (A), model of the NmCSS active site in the presence of both substrates. The conformation of CTP (green sticks) in the presence of $Ca^{2+}$(A) and $Ca^{2+}$(B) (gray spheres) superimposed into the NmCSS:CMP:Neu5Ac2en active site in which Neu5Ac2en has been replaced with Neu5Ac suggests a clash (red dashes) between $Ca^{2+}$(A) and Arg165 (thin brown sticks). However, a different rotamer of Arg165 (thick brown sticks) would allow for the observed Ca2+(A) placement while preserving the negative-charge stabilization of CTP's γ-phosphate by the arginine guanidinium group. (B), **i**, CTP binds to the nucleotide binding (NB) domain first in addition to two divalent cations. **ii**, next, Neu5Ac enters the active site and associates initially with the NB domain but quickly (**iii**) draws together the NB and dimerization domains to form the closed state (all residues involved in Neu5Ac binding are summarized below the structure for simplicity. **iv**, divalent cation $M^{2+}$ coordinates the C2-OH, allowing a water molecule to deprotonate C2-OH long enough for the hydroxyl O to attack the α-phosphate. v, after product formation, pyrophosphate ($PP_i$) and $M^{2+}$(B) are released from the active site and the active site re-opens.

180x180mm (300 x 300 DPI)

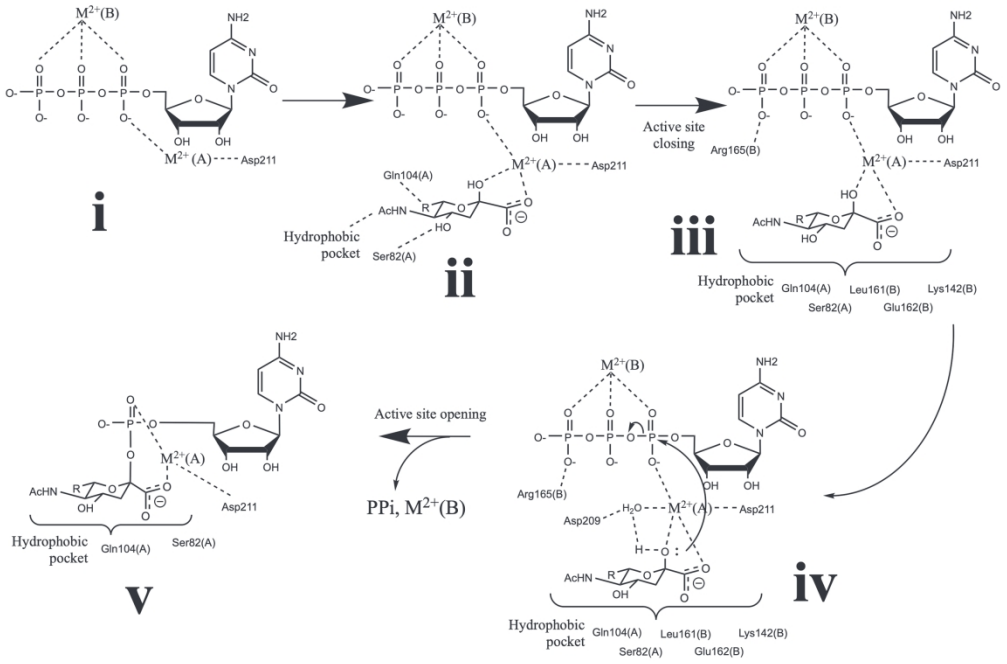


Figure 7. Proposed mechanism of NmCSS. (A), model of the NmCSS active site in the presence of both substrates. The conformation of CTP (green sticks) in the presence of $Ca^{2+}$(A) and $Ca^{2+}$(B) (gray spheres) superimposed into the NmCSS:CMP:Neu5Ac2en active site in which Neu5Ac2en has been replaced with Neu5Ac suggests a clash (red dashes) between $Ca^{2+}$(A) and Arg165 (thin brown sticks). However, a different rotamer of Arg165 (thick brown sticks) would allow for the observed Ca2+(A) placement while preserving the negative-charge stabilization of CTP's γ-phosphate by the arginine guanidinium group. (B), **i**, CTP binds to the nucleotide binding (NB) domain first in addition to two divalent cations. **ii**, next, Neu5Ac enters the active site and associates initially with the NB domain but quickly (**iii**) draws together the NB and dimerization domains to form the closed state (all residues involved in Neu5Ac binding are summarized below the structure for simplicity. **iv**, divalent cation $M^{2+}$ coordinates the C2-OH, allowing a water molecule to deprotonate C2-OH long enough for the hydroxyl O to attack the α-phosphate. v, after product formation, pyrophosphate ($PP_i$) and $M^{2+}$(B) are released from the active site and the active site re-opens.

243x160mm (300 x 300 DPI)